

4331

UNIVERSITY OF HAWAII LIBRARY

**DEVELOPMENT OF CATALYST AND  
GAS DIFFUSION LAYERS USING  
NANOTECHNOLOGY FOR PROTON  
EXCHANGE MEMBRANE FUEL CELLS**

A THESIS SUBMITTED TO THE GRADUATE DIVISION OF THE  
UNIVERSITY OF HAWAII IN PARTIAL FULFILLMENT OF THE  
REQUIREMENTS FOR THE DEGREE OF

MASTER OF SCIENCE

IN

MECHANICAL ENGINEERING

AUGUST 2008

By

Philip A. Stuckey

Thesis Committee:

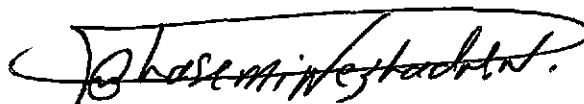
Mehrdad N. Ghasemi Nejjhad, Chairperson

Weilin Qu

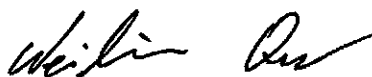
Arunachalanadar M. Kannan

We certify that we have read this thesis and that, in our opinion, it is satisfactory in scope and quality as a thesis for the degree of Masters of Science in Mechanical Engineering.

THESIS COMMITTEE

A handwritten signature in black ink, appearing to read "Joseph M. Stachurski", written over a horizontal line.

Chairperson

A handwritten signature in black ink, appearing to read "William R. ...", written over a horizontal line.A handwritten signature in black ink, appearing to read "D. ...", written over a horizontal line.

## **ACKNOWLEDGEMENTS**

I would like to recognize and thank my advisor, Dr. Mehrdad N. Ghasemi Nejjhad for his guidance, expertise, and support throughout my graduate studies. I would also like to thank Dr. A. M. Kannan from Arizona State University Polytechnic Campus for his guidance in fuel cell testing and use of Alternative Energy Laboratory during my numerous visits. I also thank Dr. Weilin Qu for serving on my defense committee and Dr. Anyuan Cao for sharing his passion of nanotechnology. I cannot forget to mention my parents, family, and friends, including those in the Hawaii Nanotechnology Laboratory, because without their support, I would not have made it this far.

# TABLE OF CONTENTS

ACKNOWLEDGEMENTS.....	iii
LIST OF FIGURES .....	vi
ABSTRACT.....	viii
CHAPTER 1 INTRODUCTION .....	1
1.1 Operation of Proton Exchange Membrane Fuel Cell.....	1
1.2 Typical Fuel Cell Design .....	3
1.3 Losses in Fuel Cell Operation.....	4
1.4 Water Management, Humidification, and Temperature Needs for Proton Exchange Membrane Fuel Cells .....	4
1.5 Conclusions.....	5
CHAPTER 2 DEVELOPMENT OF <i>IN-SITU</i> MODIFIED CARBON PAPERS WITH MULTI-WALLED CARBON NANOTUBES USED AS GAS DIFFUSION LAYERS FOR PROTON EXCHANGE MEMBRANE FUEL CELLS.....	6
2.1 Overview.....	6
2.2 Introduction.....	7
2.3 Experimental Methodology .....	8
2.4 Results and Discussion .....	10
2.5 Conclusions.....	19
CHAPTER 3 IMPROVED CATALYST LAYERS FOR PROTON EXCHANGE MEMBRANE FUEL CELLS USING UNIFORMLY DISPERSED PLATINUM NANOPARTICLES SUPPORTED ON MULTI-WALLED CARBON NANOTUBES	21
3.1 Overview.....	21
3.2 Introduction.....	21
3.3 Experimental .....	23
3.3.1 Multi-Walled Carbon Nanotube Growth .....	23
3.3.2 Process 1- Process from Prior Work.....	23
3.3.3 Process 2- New Improved Process.....	24
3.3.4 Fuel Cell Testing.....	24
3.4 Results and Discussion .....	25
3.5 Conclusions.....	30
CHAPTER 4 NOVEL USE OF PLATINUM NANO-WIRES AS A CATALYST FOR PROTON EXCHANGE MEMBRANE FUEL CELLS .....	31
4.1 Overview.....	31
4.2 Introduction.....	31
4.3 Experimental.....	32
4.3.1 Experimental Overview .....	32
4.3.2 Procedure for Hot Pressing .....	32
4.3.3 Procedure for Micro-Spray Technique .....	33
4.3.4 Fuel Cell Testing.....	33
4.4 Results and Discussion .....	34
4.5 Conclusions.....	41
CHAPTER 5 GENERAL CONCLUSIONS.....	42

<b>APPENDIX. POLARIZATION CURVES FOR THE DEVELOPMENT OF IN-SITU MODIFIED CARBON PAPERS WITH MULTI-WALLED CARBON NANOTUBES USED AS GAS DIFFUSION LAYERS FOR PROTON EXCHANGE MEMBRANE FUEL CELLS .....</b>	<b>44</b>
<b>REFERENCES .....</b>	<b>58</b>

# LIST OF FIGURES

Figure 1.1. Schematic of the location and reactions in a fuel cell. ....	2
Figure 1.2. Fuel cell structure showing the location of the membrane electrode assembly (MEA) and other components.....	3
Figure 2.1. SEM showing the surface morphology of the as-received carbon paper (inset shows a close-up of bare carbon fibers).....	11
Figure 2.2. SEM showing the surface morphology of the in-situ modified carbon paper (inset shows close-up view of the in-situ grown MWCNTs nanoforests on the carbon fibers). ....	12
Figure 2.3. SEM of the in-situ grown MWCNT nanoforest on carbon paper showing the presence of multi-walled carbon nanotubes on the in-situ modified carbon paper. ....	13
Figure 2.4. TEM of the in-situ grown MWCNTs scraped off the carbon paper showing the presence of multi-walled carbon nanotubes on the in-situ modified carbon paper. ...	14
Figure 2.5. Contact angle image from water drop test showing a contact angle of 147° for the as-received carbon paper. ....	15
Figure 2.6. Contact angle image from water drop test showing a contact angle of 168° for the in-situ modified carbon paper. ....	16
Figure 2.7. Peak power density for gas diffusion layers testing the as-received carbon paper and the in-situ modified carbon paper in the H <sub>2</sub> /O <sub>2</sub> proton exchange membrane fuel cell system. ....	18
Figure 2.8. Peak power density for gas diffusion layers testing the as-received carbon paper and the in-situ modified carbon paper in the H <sub>2</sub> /Air proton exchange membrane fuel cell system ....	19
Figure 3.1. TEM micrograph showing the platinum nanoparticles distribution on MWCNTs from prior work using Process 1 <sup>21</sup> . ....	27
Figure 3.2. TEM micrograph showing the platinum nanoparticle distribution on MWCNTs from current work using refined procedures via Process 2.....	28
Figure 3.3. Galvanostatic polarization and power density plots for testing Pt/MWCNT catalyst. ....	29
Figure 4.1. SEM image of the as-grown platinum nanowires on silicon substrate showing the porous nature of this nanostructure from the top view. ....	35
Figure 4.2. SEM image of the as-grown platinum nanowires on silicon substrate showing the porous nature of this nanostructure from the side view. ....	36
Figure 4.3. SEM cross-sectional view of platinum nanowires on Nafion® NRE-211 taken at a 45° stage tilt showing the lead film covering the nanowires and the cracks in the metallic film. ....	37
Figure 4.4. SEM cross-sectional view of platinum nanowires on Nafion® NRE-211 taken at a 45° stage tilt showing the aligned structure of the nanowires.....	38
Figure 4.5. Fuel cell voltage and power density measured by galvanostatic polarization comparing a cell made with the platinum nanowires on the anode to a fuel cell made with commercially available catalyst. ....	39

Figure 4.6. SEM of as-received platinum nanowires detached from the substrate showing a thin metallic layer at the base of the platinum nanowire forest. ....	40
Figure 4.7. Elemental analysis showing the presence of platinum and lead in the SEM images. ....	41
Figure A.1.1 100% RH, 24% peak power improvement, -1% voltage improvement at peak power density. ....	45
Figure A.1.2. 90% RH, 3% peak power improvement, -2% voltage improvement at peak power density. ....	46
Figure A.1.3. 80% RH, 9% peak power improvement, 2% voltage improvement at peak power density. ....	47
Figure A.1.4. 70% RH, 21% peak power improvement, 5% voltage improvement at peak power density. ....	48
Figure A.1.5. 60% RH, 43% peak power improvement, -12% voltage improvement at peak power density. ....	49
Figure A.1 6. 50% RH, 155% peak power improvement, 14% voltage improvement at peak power density. ....	50
Figure A.2.1 100% RH, -6% peak power improvement, -3% voltage improvement at peak power density. ....	51
Figure A.2.2. 90% RH, 4% peak power improvement, -5% voltage improvement at peak power density. ....	52
Figure A.2.3. 80% RH, 5% peak power improvement, -5% voltage improvement at peak power density. ....	53
Figure A.2.4. 70% RH, 3% peak power improvement, -11% voltage improvement at peak power density. ....	54
Figure A.2.5. 60% RH, 43% peak power improvement, 9% voltage improvement at peak power density. ....	55
Figure A.2.6. 50% RH, 86% peak power improvement, 15% voltage improvement at peak power density. ....	56
Figure A.2.7. 40% RH, 157% peak power improvement, 16% voltage improvement at peak power density. ....	57

# ABSTRACT

Nanotechnology in Proton Exchange Membrane Fuel Cells (PEMFCs), the topic of this thesis, encompasses a large array of subjects. It is important to understand the market demand for fuel cells and then realize the types of changes and improvements of the technology needed to bring it to the marketplace. By integrating nanotechnology into fuel cells, their performances will be greatly increased. Nanotechnology will be able to provide the profound material properties of nanoscaled materials and structures needed to make fuel cells a desired technology. Novel gas diffusion layers (GDLs) and catalyst layers (CLs) have been developed for PEMFCs in this work. Carbon nanotubes (CNTs) are grown directly and in-situ on carbon papers to develop high performance durable GDLs that can operate at high temperature and low humidity during fuel cell testing. Platinum nanoparticles are combined with CNTs using a new chemical processing route to develop efficient and lower cost CLs confirmed by fuel cell testing. In addition, platinum nanowires were employed for the development of catalyst layers; however, due to the manufacturing of platinum nanowires and their substrate, necessary to hold them vertically, the fuel cell tests did not show promising results and further work is recommended for future studies to utilize the full potentials of platinum nanowires.

# CHAPTER 1

## INTRODUCTION

### 1.1. Operation of Proton Exchange Membrane Fuel Cell

A fuel cell is an electrochemical device that combines a fuel and air to directly produce electrical power. If pure hydrogen is used as a fuel in a proton exchange membrane fuel cell (PEMFC), the only products of this process are heat, electricity, and water<sup>1</sup>.

A PEMFC consists of a polymer electrolyte positioned between two electrodes. The electrolyte allows positive ions to pass through the medium while inhibiting the flow of electrons. In the case of the hydrogen fuel cell, the positive ions are merely protons ( $H^+$ ). As hydrogen gas passes over an anode in fuel cell system (see Figure 1.1), a catalyst assists in separating hydrogen into electrons and protons as shown in the following reaction<sup>1</sup>:



Rather than flowing through the membrane, like the hydrogen protons, the electrons flow to the other electrode, the cathode, through an external circuit, thus creating electricity (see Figure 1.1). As both electrons and protons meet at the cathode, oxygen or air is flown over the cathode in the presence of a catalyst producing water<sup>1</sup>:



The reactants and products at the anode and cathode are represented in one overall reaction<sup>1</sup>:



which is merely the production of water from elemental hydrogen and oxygen. The location of the above reactions is visualized in Figure 1.1. In this figure, the anode and cathode are also called the gas diffusion layers (GDLs). The catalyst layers (CLs) are in between the GDLs and the electrolyte.

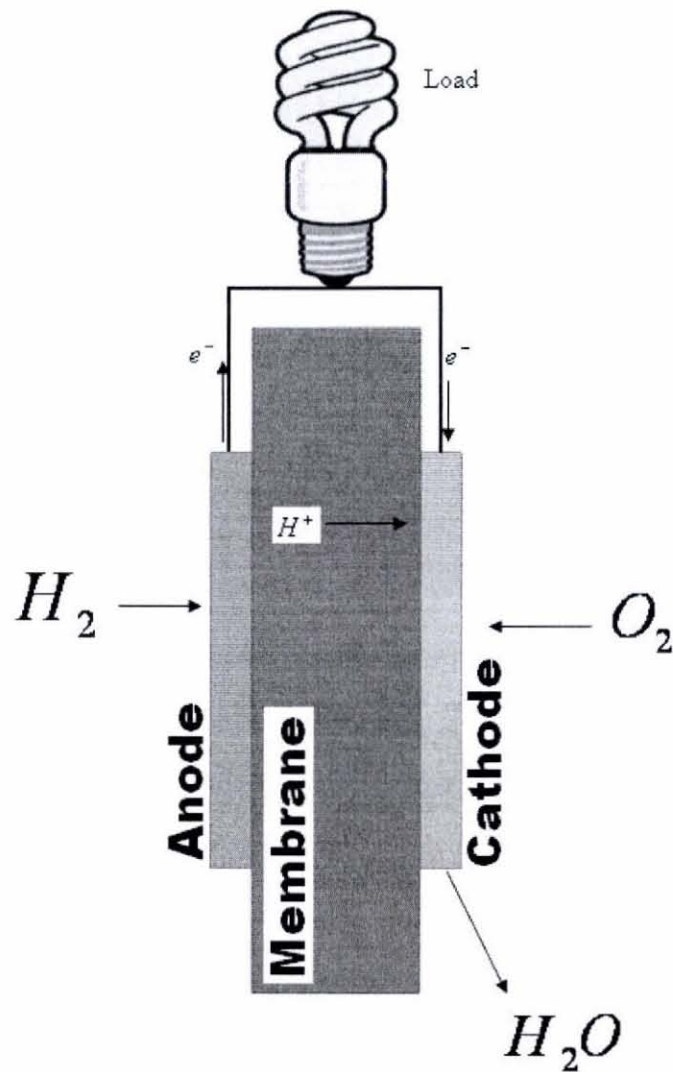


Figure 1.1. Schematic of the locations and reactions in a fuel cell.

## 1.2. Typical Fuel Cell Design

Three of the components discussed above, i.e. a catalyst layer, polymer electrolyte, and a catalyst layer, when sealed together form the membrane electrolyte assembly (MEA) as shown in Figure 1.2. Positioned against the MEA are the gas diffusion layers (GDLs) – a porous media that assists in exchanging reactant and product gases at the catalyst layers, managing the water content in the fuel cell, and completing the electronic circuit functioning as the anode and cathode. Gaskets are used in the fuel cell to provide gas sealing from the atmosphere. Since the dimensions of the polymer membrane are larger than the catalyst layers and GDLs, the gaskets also account for the difference in thickness for the GDLs and catalyst layers. Bipolar plates, commonly made from graphite, have gas flow channels machined into the thickness of the material to deliver the reactant and product gases.

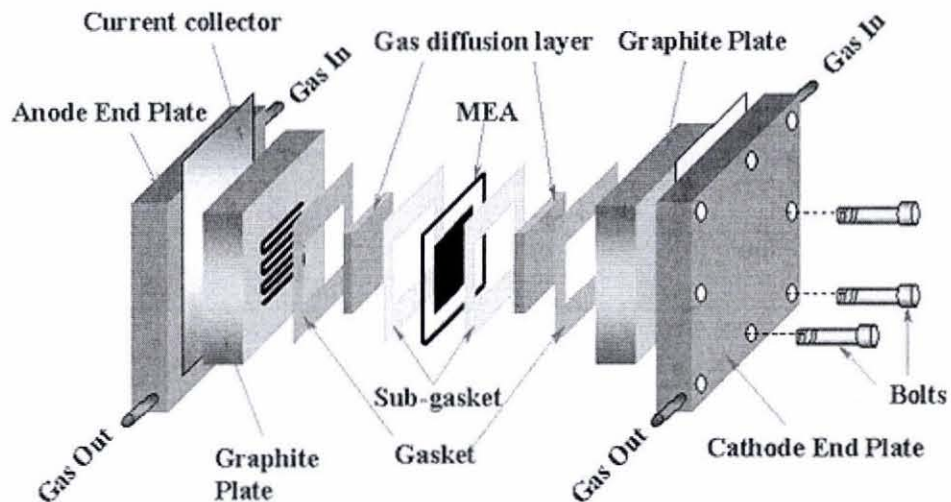


Figure 1.2. Fuel cell structure showing the location of the membrane electrode assembly (MEA) and other components.

### **1.3. Losses in Fuel Cell Operation**

There are three main voltage drops in fuel cells: activation losses, ohmic losses, and concentration losses<sup>1</sup>. Activation losses originate from the need to move electrons from the anode to the cathode and the energy to break and form chemical bonds in the anode and cathode. Ohmic losses are caused by the resistance inherent in the polymer membrane's ability to transfer the protons from the anode to the cathode and the resistance of the other components in the fuel cell that are involved in transferring electrons. Concentration losses, often called mass transport losses originate from the decrease in concentration of the reactants at the catalyst sites as they are consumed by the reactions. Since the rate of reactant/fuel consumption must be high for this loss to occur, the rapid loss of voltage is only seen at high current densities<sup>1</sup>.

### **1.4. Water Management, Humidification, and Temperature Needs for Proton Exchange Membrane Fuel Cells**

For effective performance and efficiency, the water content in a PEMFC must be carefully controlled and many details must go into the design of the fuel cells. The polymer membrane absorbs water which is needed for proton conduction through the membrane. Insufficient water content will result in a decrease or failure in performance<sup>2</sup>. Other components in the fuel cell, such as the gas diffusion layers and catalyst layers have porous structures and too much water will result in flooding, thus blocking the flow of gasses in the fuel cell resulting in a decrease in efficiency or a complete failure in performance<sup>3</sup>.

Water management and humidification becomes even more complex given that PEMFCs are typically operated at higher temperatures (i.e., 60 - 90 °C) to improve efficiency<sup>4</sup>. At these temperatures, external humidification of reactant gases before entering the fuel cell is needed otherwise the fuel cell will become too dry causing performance to suffer<sup>5</sup>.

Humidifying reactant gases for a fuel cell is difficult and depending on the size of the system often requires extra equipment such as humidifiers, water separators, and heating coils. These increase the overall size of the system, consume part of the power produced by the system, and thus decrease the efficiency and power output by the fuel cell system<sup>6</sup>.

## **1.5. Conclusions**

This thesis attempts to elaborate on the complexity depth of the materials, design, manufacture, costs, and markets for PEMFC. Fuel cells are extremely complex and improvements that result in higher performance coupled with simpler design are certainly warranted. Nanotechnology applications may indeed have a profound impact on the fuel cell industry.

## **CHAPTER 2**

# **DEVELOPMENT OF *IN-SITU* MODIFIED CARBON PAPERS WITH MULTIWALLED CARBON NANOTUBES USED AS GAS DIFFUSION LAYERS FOR PROTON EXCHANGE MEMBRANE FUEL CELLS**

### **2.1. Overview**

Gas diffusion layers (GDLs) enhance the delivery of gases to the catalyst layers by controlling the water in the pore channels while simultaneously completing the electronic circuit needed to deliver the power generated by the fuel cell. Current carbon paper products for the GDL offer limited hydrophobic characteristics which are often enhanced by a Teflon® poly(ethylene terephthalate) PTFE coating on the surfaces of the carbon paper. In this work, we report the in-situ growth of carbon nanotubes directly onto carbon papers. This modification enhances both the hydrophobic nature of the carbon papers as well as their porosity in the fuel cell. The development of in-situ modified carbon paper with carbon nanotubes creates an extremely hydrophobic surface verifiable through measuring contact angle by the water drop method. The developed in-situ modified carbon papers are used as GDLs in a fuel cell and show no performance loss when operated at elevated temperatures with lower humidity conditions, demonstrating a marked improvement for fuel cell performance under these conditions, when compared to the current state-of-the-art.

## 2.2. Introduction

Proton exchange membrane fuel cells (PEMFCs) are emerging as power providing devices for stationary and portable devices<sup>7-8</sup>. To achieve higher operating efficiencies, PEMFCs are operated at elevated temperatures, around 70°C. Operation at this elevated temperature requires extensive humidification of gases, particularly when using ambient air at the cathode<sup>9-10</sup>. Reducing the humidification requirements increases the efficiency by allowing simplified humidification methods. Gas diffusion layers (GDLs) have been developed to manage water in the cell as well as promote gas flow to the active catalyst. For several years, carbon papers with PTFE coatings have been the major choice for GDLs<sup>11</sup>. Other reports have seen performance increases by creating micro-porous layers on the carbon paper<sup>12-13-14</sup>. While this process is effective, it requires additional ex-situ steps to apply additional carbon and PTFE material onto the surfaces of carbon paper, substantially increasing the thickness of the carbon paper. When designing compact fuel cells, this extra thickness could increase the size of a fuel cell stack. Other examples of modifying gas diffusion layers have combined carbon cloths with other carbon loading to achieve similar ex-situ results discussed above<sup>15</sup>.

Carbon nanotubes have been touted for a wide range of energy applications with interesting properties<sup>16</sup>. Since multi-walled carbon nanotubes (MWCNTs) can transport large currents with low resistance<sup>17</sup>, this property could be highly desirable at the electrode surfaces in a PEMFC. Carbon nanotube forests have extremely hydrophobic

properties<sup>18</sup> as well as an inherent structure that resists oxidation<sup>19</sup>. These properties are highly desirable in the harsh environments found inside fuel cells.

### **2.3. Experimental Methodology**

The as-received carbon paper (GD07508T, Hollingsworth and Vose Company, West Groton, MA) was cut into pieces small enough to fit into a furnace (F79300, Barnstead International) configured for chemical vapor deposition (CVD) for the *in-situ* growth of MWCNT nanoforests. The carbon paper pieces were loaded into the heating zone of a quartz tube of a CVD furnace and heated to 770 °C in an argon atmosphere. A mixture of 1 wt% ferrocene (Aldrich F408), in xylenes (Fisher X5), was used as a catalyst in carbon source, respectively, for the *in-situ* MWCNT growth over the carbon paper. The developed in-situ modified carbon paper was directly assembled as the GDL in the PEMFC. Both the as-received and in-situ modified carbon papers were analyzed using the scanning electron microscope. To further confirm the presence of multi-walled carbon nanotube nanoforests on the surface of the in-situ modified carbon paper, some material was scraped from the surface, dispersed in DI water, and loaded onto a lacy carbon grid for transmission electron microscopy.

Catalyst coated membranes (CCMs) with 5 cm<sup>2</sup> active area were fabricated using platinum supported on carbon made into catalyst slurry. The slurry was made by purging the catalyst powder in flowing nitrogen gas for 30 minutes to avoid any decomposition. The slurry was applied to a Nafion® NRE-211 membrane (Ion Power Inc, New Castle,

DE) using a micro-spray technique. To improve the “3-phase contact” of the reaction zone<sup>20</sup> (i.e., solid membrane/catalyst layer, liquid water in the electrolyte, and gas reactants), 15 wt% Nafion® solution (LQ-1115, Ion Power Inc, New Castle, DE) was added to the slurry using a ratio of 2 ml of 15 wt% liquid Nafion to 20 ml of isopropanol. The CCM was dried in a vacuum oven at 50°C for 30 minutes.

The GDLs and the CCM were assembled in a single test cell (Fuel Cell Technologies, Albuquerque, NM, USA) by sandwiching them together with silicone-coated fabric (CF1007, Saint-Gobain Performance Plastics) to provide gas sealing. The cell was closed and tightened to a uniform torque of 40 lb-in. The cell performance was tested using galvanostatic polarization with Greenlight Test Station (G50 Fuel Cell System, Hydrogenics, Vancouver, Canada). The cell was purged with nitrogen and tested at 70°C with H<sub>2</sub>/O<sub>2</sub> and H<sub>2</sub>/air. Hydrogen gas was flowed over the anode at a rate of 0.2 SCCM and oxygen or air was flowed over the cathode at a rate of 0.4 SCCM. The humidity in the cell was controlled by adjusting the humidity bottle temperature. Starting at the lower relative humidity value, the humidity of the fuel cell reactant gases was increased in 10% increments allowing 2 hours for membrane conditioning to occur. Once 100% relative humidity was reached, the tests were repeated while decreasing the humidity to ensure consistency in the data. The cell temperature was controlled using a resistive heater inside the end plates. Two cells were tested using this method, one cell with the in-situ modified carbon paper used as the GDL and the other cell using the plain, as-received carbon paper as the GDL. All other components in the fuel cell were the same to provide an experimental cell that can be compared to a reference cell.

## **2.4. Results and Discussion**

The process used to in-situ modify the carbon paper was that of a CVD process. Figure 2.1 shows SEM images of the plain, as-received carbon paper compared to the in-situ modified carbon paper shown in Figure 2.2.

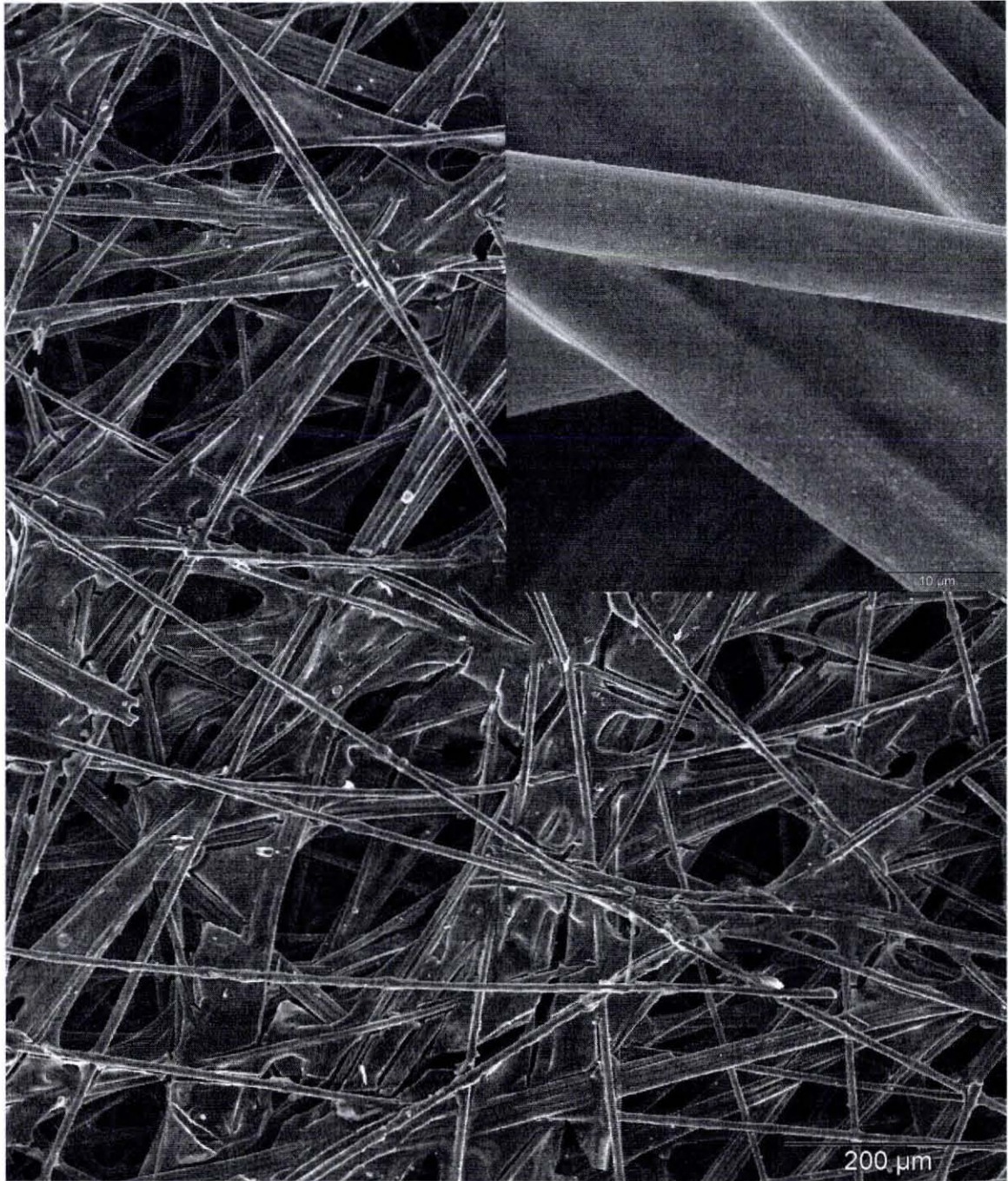


**Figure 2.1. SEM showing the surface morphology of the as-received carbon paper (inset shows a close-up of bare carbon fibers).**

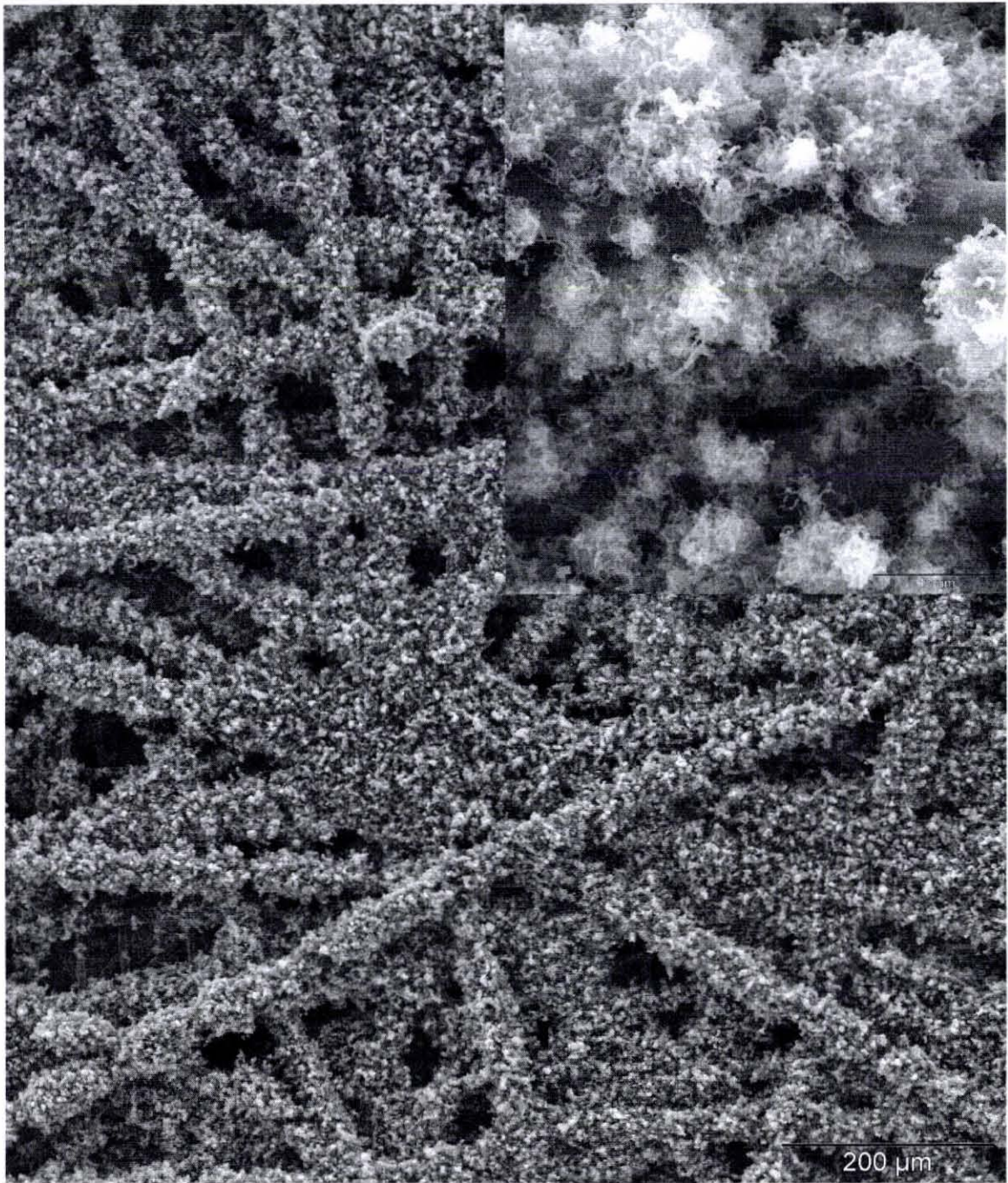
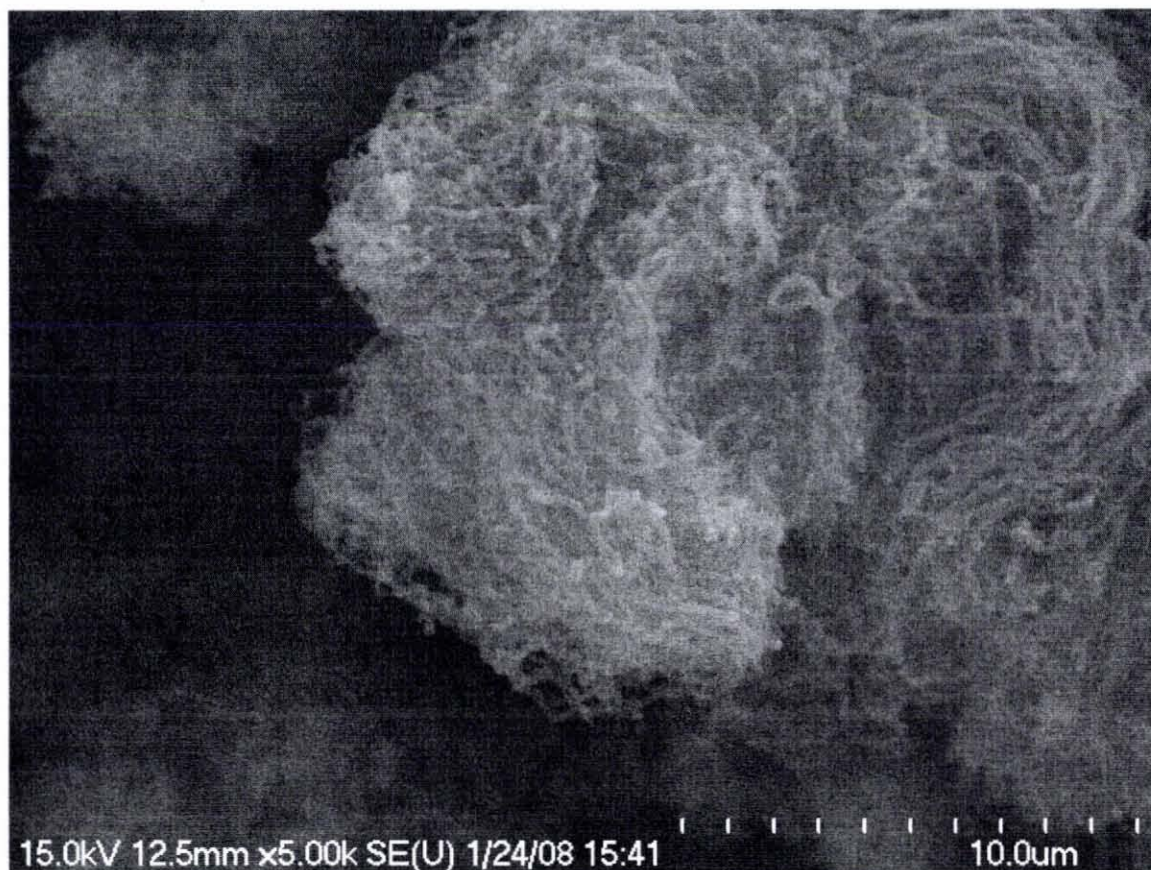
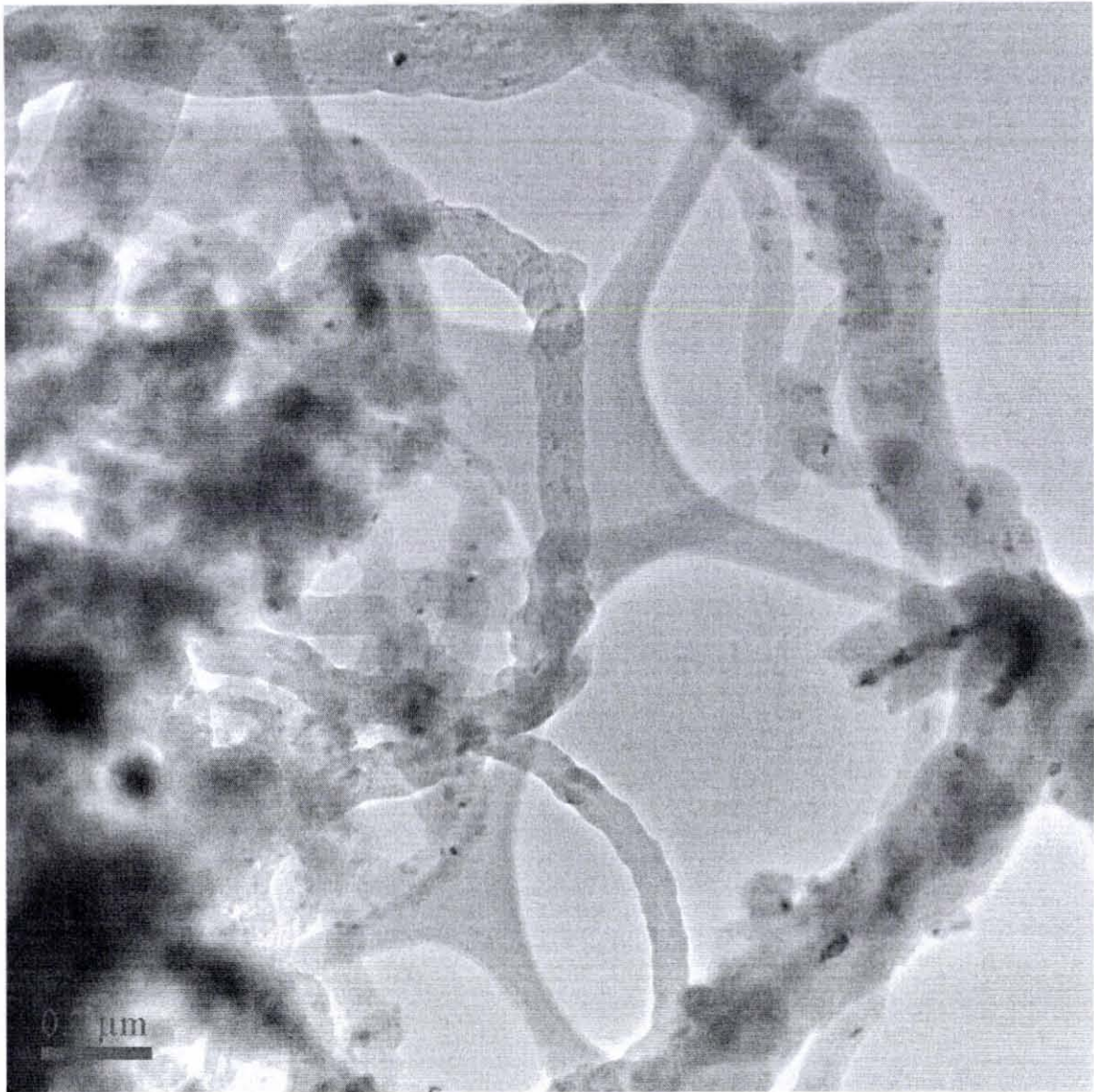


Figure 2.2. SEM showing the surface morphology of the in-situ modified carbon paper (inset shows close-up view of the in-situ grown MWCNTs nanoforests on the carbon fibers).

The in-situ modification consists of the growth of MWCNTs on the surface of as-received carbon paper. The presence of MWCNTs resembles nanoforest and is confirmed by the SEM and TEM micrographs in Figures 2.3 and 2.4, respectively.



**Figure 2.3. SEM of the in-situ grown MWCNT nanoforest on carbon paper showing the presence of multi-walled carbon nanotubes on the in-situ modified carbon paper.**



**Figure 2.4. TEM of the in-situ grown MWCNTs scraped off the carbon paper showing the presence of multi-walled carbon nanotubes on the in-situ modified carbon paper.**

Since carbon nanotube nanoforests, grown on the surface of the carbon paper, are hydrophobic in nature, their presence on the surface of the in-situ modified carbon paper promotes hydrophobic properties. This observation is justified by measuring the contact

angle for the as-received paper and comparing it to that for the in-situ modified carbon paper. The plain as-received teflonized carbon paper exhibits a contact angle of  $147^\circ$  (see Figure 2.5) which is lower than the contact angle of  $168^\circ$  (see Figure 2.6) exhibited by the in-situ modified carbon paper. The heating, during the CVD process, causes the Teflon coating to evaporate from the surface of the carbon paper.

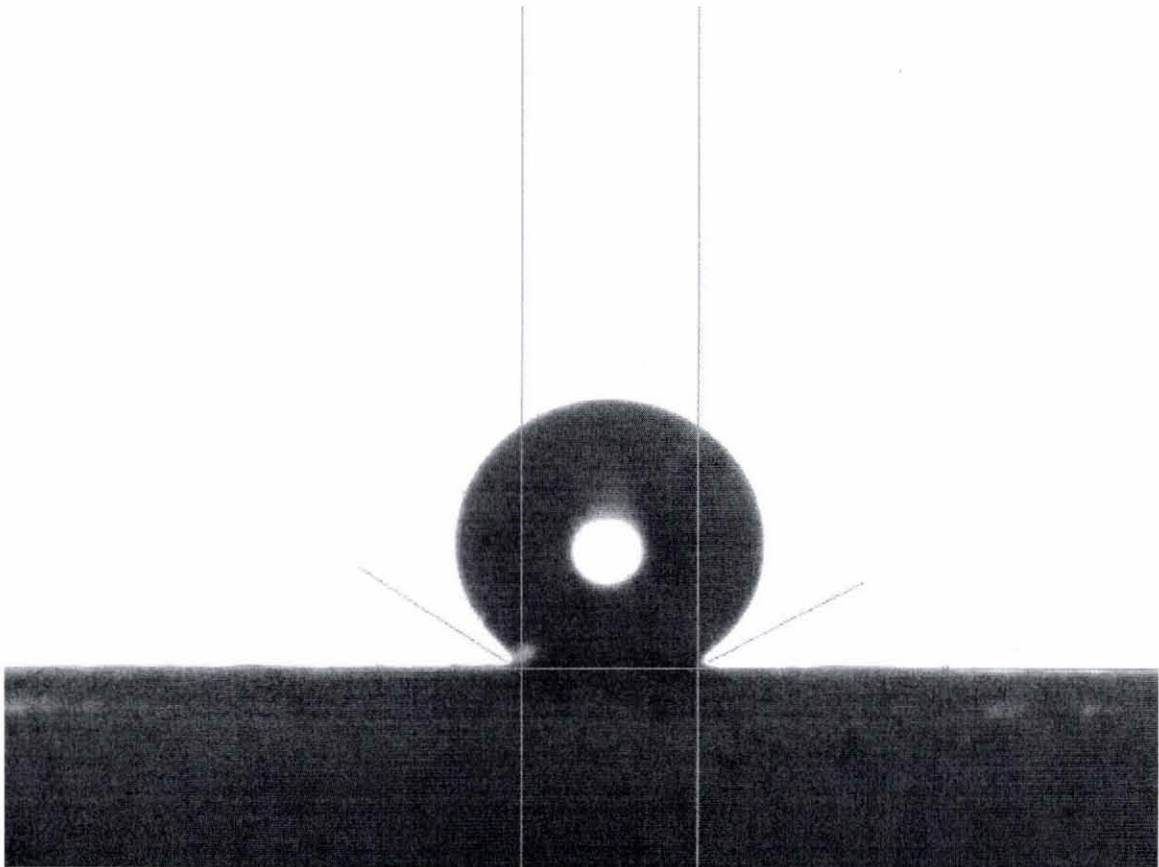


**Figure 2.5. Contact angle image from water drop test showing a contact angle of  $147^\circ$  for the as-received carbon paper.**

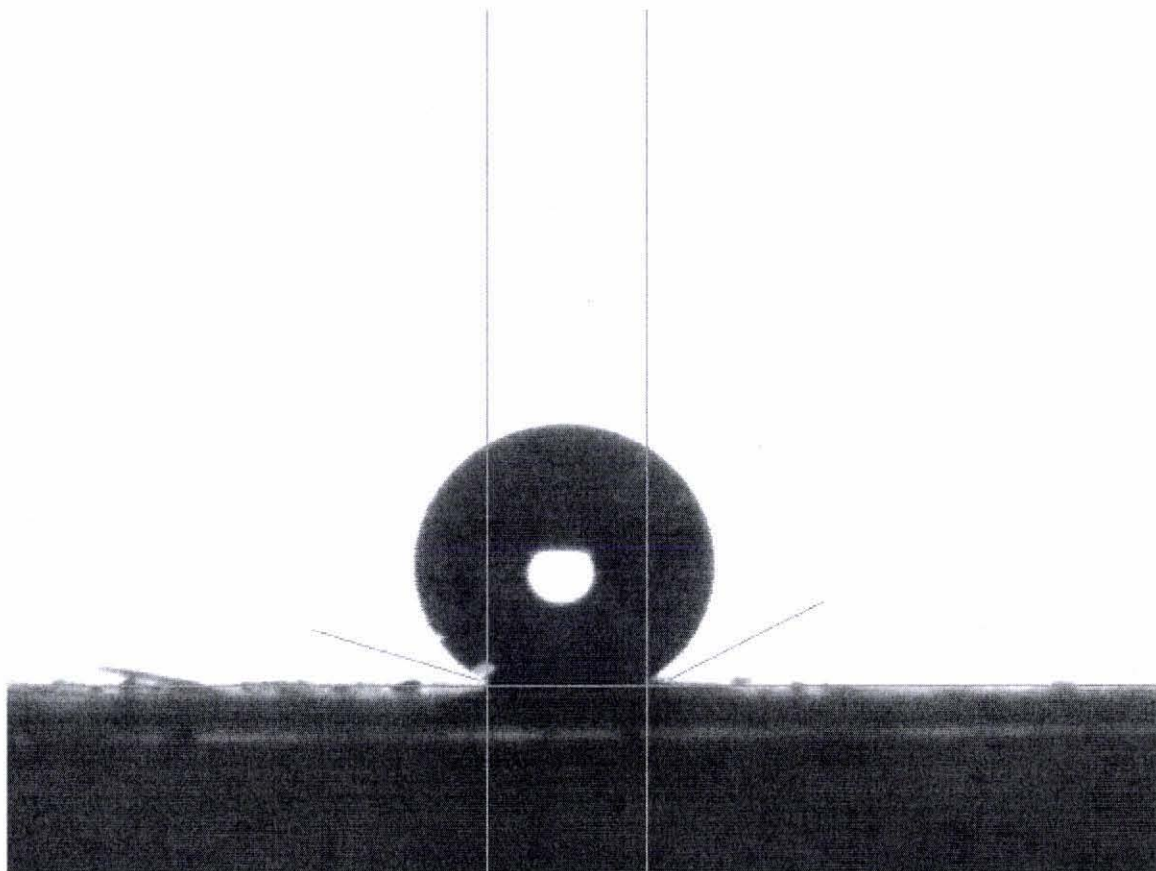


**Figure 2.6. Contact angle image from water drop test showing a contact angle of  $168^\circ$  for the in-situ modified carbon paper.**

Polarization curves were generated while operating the cell at varying relative humidity (RH) values and the peak power density from each curve was generated and plotted in Figures 2.7 and 2.8 for  $H_2/O_2$  and  $H_2/Air$ , respectively. The polarization curves corresponding to each data point are provided in the Appendix. It can be observed in figures provided in the Appendix that as the RH decreases the behavior of as-received carbon paper fuel cell becomes unstable; whereas the in-situ modified carbon paper fuel cell demonstrates stability as the RH decreases. The trend shows that the performance of the cell using the as-received carbon paper is best at high humidity conditions, i.e., 100-

70% relative humidity and the fuel cell performance falls with relative humidity below 70%. The in-situ modified carbon paper, on the other hand, shows sustained performance at both high and low humidity conditions in the testing range of 100–40% relative humidity. When comparing the peak power density of the in-situ modified carbon paper fuel cell to the as-received carbon paper fuel cell, a performance increase of 155% is noticed for the operation in H<sub>2</sub>/O<sub>2</sub> at 50% RH (see Figure 2.7) and a performance increase of 157% is noticed for the operation in H<sub>2</sub>/Air at 40% RH (see Figure 2.8). The performance increase at the lower relative humidity conditions for the *in-situ* modified carbon papers is due to the presence of the hydrophobic layer consisting of multi-walled carbon nanotubes nanoforests, grown in-situ, which repels the water from the gas diffusion layer, and hence prevents the flooding of the GDLs and promotes the membrane hydration while still promoting gas exchange across the catalyst layer. Higher membrane hydration promotes proton conductivity across the membrane from the anode to the cathode. This modification illustrates a novel method of using multi-walled carbon nanotubes to improve the performance of proton exchange membrane fuel cells.

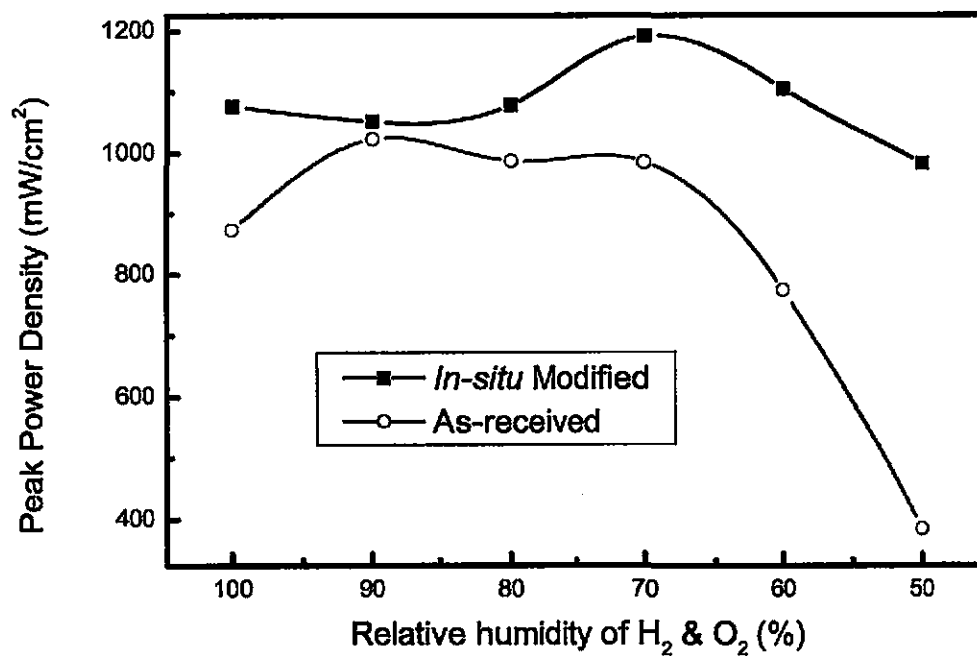


**Figure 2.7. Peak power density for gas diffusion layers testing the as-received carbon paper and the in-situ modified carbon paper in the H<sub>2</sub>/O<sub>2</sub> proton exchange membrane fuel cell system.**

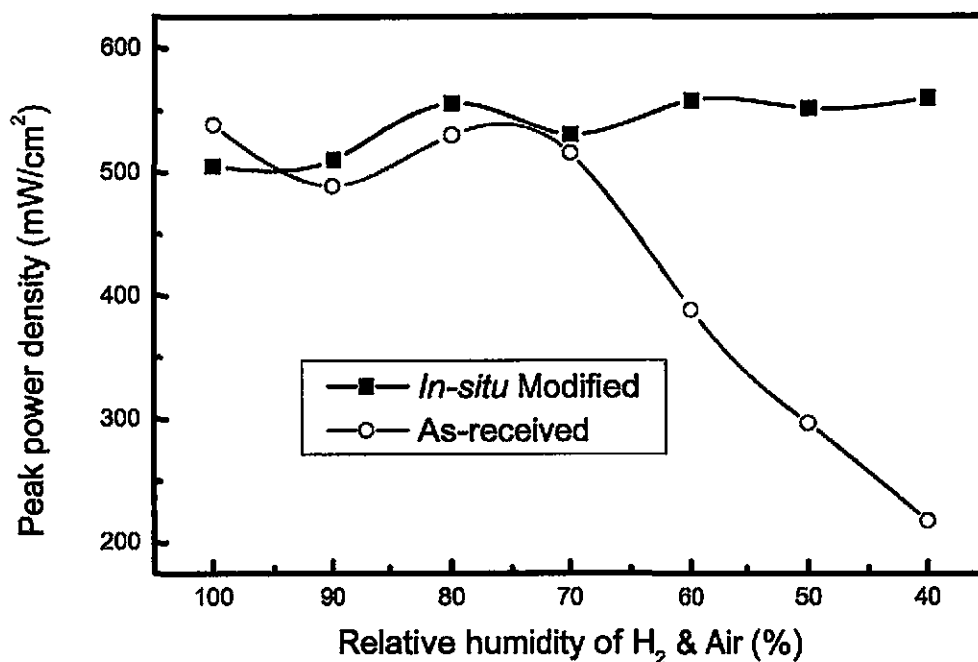


**Figure 2.8. Peak power density for gas diffusion layers testing the as-received carbon paper and the in-situ modified carbon paper in the H<sub>2</sub>/Air proton exchange membrane fuel cell system**

## 2.5. Conclusions

The in-situ modified carbon paper with the direct growth of carbon nanotubes shows excellent performance over a wide range of humidity conditions, including lower humidity when compared to plain as-received teflonized carbon paper. The performance of fuel cells that operate with atmospheric air, unstable humidity conditions, or with simplified humidification systems could be significantly enhanced using the in-situ gas diffusion layer developed here. To fully realize the potentials of the gas diffusion layer

developed here, a long-term durability test should be conducted to ensure continuous operation.

# **CHAPTER 3**

## **IMPROVED CATALYST LAYERS FOR PROTON EXCHANGE MEMBRANE FUEL CELLS USING UNIFORMLY DISPERSED PLATINUM NANOPARTICLES SUPPORTED ON MULTI-WALLED CARBON NANOTUBES**

### **3.1. Overview**

Multi-walled carbon nanotubes are used as a robust nano-structure component for the deposition of platinum nanoparticles via an aqueous acidic reduction process. Scanning electron micrographs show superior dispersion of platinum nanoparticles with consistent particle size (2-4 nm) on multi-walled carbon nanotubes compared to prior work in this area<sup>21</sup>. This improvement is achieved by introducing a new process in this work. Furthermore, fuel cell testing shows that the newly developed nanocomponent serves as a viable catalyst layer for proton exchange membrane fuel cells.

### **3.2. Introduction**

When a PEMFC is fed with hydrogen and oxygen, catalysts are needed to initiate the chemical reactions<sup>1</sup>. Solid oxide fuel cells overcome this problem by operating at higher temperatures (e.g., at 650-1000 °C)<sup>1</sup>. Platinum has been found to be the best catalyst for this application<sup>1</sup> but conservation of this metal is required to bring down the costs and

increase the performance of PEMFCs. Loading the electrodes of the fuel cell with platinum black is extremely inefficient, requiring around 28 mg of Pt/cm<sup>2</sup><sup>1</sup> and was quickly replaced with more efficient methods leading to a new area of research to load platinum onto other materials (such as graphitic carbon)<sup>1</sup> thereby decreasing the mass of platinum used per square centimeter to around 0.2 mg of Pt/cm<sup>2</sup>; however, after extended periods of operation, carbon supports tend to degrade<sup>1</sup>. Thus, it is obvious that the use of platinum black is an inefficient use of platinum; however, there must be enough platinum present to ensure adequate reaction sites, hence ultra low platinum loading on carbon supports is also inefficient. Increasing the platinum loading on carbon support from 20 wt% to 50 wt% reduces the amount of material needed to make a functioning electrode and thus reduces the thickness of the catalyst layer needed to fabricate a functioning membrane electrode assembly (MEA). A thinner catalyst layer results in a shorter distance for proton diffusion through the membrane as well as shorter diffusion lengths for reactant and exhaust gases.

Carbon nanotubes have an inherent structure that resists oxidation<sup>22</sup>, and therefore multi-walled carbon nanotubes (MWCNTs) are promising materials to withstand the harsh environments inside PEMFCs. Prior attempts<sup>13 21-24</sup> of improving and controlling the dispersion of platinum nano-particles on MWCNTs have not fully achieved the distribution observed using the process introduced here.

### **3.3. Experimental**

#### ***3.3.1. Multi-Walled Carbon Nanotube Growth***

MWCNTs were prepared using a chemical vapor deposition furnace (Barnstead International F79300) at 770 C in an argon atmosphere using ferrocene (Aldrich F408) as a catalyst and xylenes (Fisher X5) as the carbon source in a ratio of 1g per 100 ml, respectively. Silicon wafers with a thermal oxide layer were used as the substrate for MWCNTs growth. MWCNTs were then scraped from the substrate and stored in a container for experimental use.

#### ***3.3.2. Process 1- Process from Prior Work***

In our previous work<sup>21</sup>, MWCNTs were dissolved in deionized water. The solution was ultrasonically dispersed for about 2 hours, until the bundles of MWNCTs were visually separated. The solution was filtered using a Buchner funnel with a pore size of 4-5.5  $\mu\text{m}$  and washed with deionized water. The washed MWCNT were redispersed in deionized water and magnetically stirred at  $\sim 70$  °C. Chloroplatinic acid hydrate (Sigma 81080) and sodium formate were diluted in 0.250 L of respective solute using different separatory funnels. These two solutions were added drop wise into a beaker containing the stirring MWCNT solution. The obtained solution contained platinum coated MWCNTs and sodium salt. The solution was filtered through a Buchner funnel (pore size of 4-5.5  $\mu\text{m}$ ) to separate the salt and collect the remaining Pt/MWCNT.

### ***3.3.3. Process 2- New Improved Process***

In a round bottom flask filled half way with deionized water, MWCNTs and Chloroplatinic acid hydrate (Sigma 81080) were added to achieve 50% Pt weight loading on the 50% by weight MWCNTs. The mixture was ultrasonically mixed for 30 minutes and stirred by hand every 10 minutes, until the bundles of MWCNTs were visually separated, which typically took about 2 hours. The solution was then heated just to a boil and the boiling was suppressed by magnetic stirring. In a separate container, 1.5 g of sodium formate was diluted in de-ionized water and slowly added drop wise to the stirring solution. The solution was stirred overnight to ensure that all the chloroplatinic acid hydrate had been reduced. The remaining solution contained platinum coated MWCNTs and sodium salt. With the platinum on the MWCNTs, the solution was gravity filtered using an ashless Whatman filter without any vacuum. The Pt/MWCNT sample was repeatedly washed with warm de-ionized water and then scraped from the filter.

### ***3.3.4. Fuel Cell Testing***

Catalyst coated membranes (CCMs) with a 5 cm<sup>2</sup> active area were fabricated using platinum supported on carbon made into catalyst slurry. The slurry was produced by purging the catalyst powder in flowing nitrogen gas for 30 minutes to avoid any decomposition. The slurry was applied to a Nafion® NRE-211 membrane (Ion Power Inc, New Castle, DE) using a micro-spray technique. To improve the “3-phase contact”

of the reaction area (i.e., the solid catalyst/membrane, the liquid water in the electrolyte, and the gas reactants<sup>20</sup>), 15 wt% Nafion® solution (LQ-1115, Ion Power Inc, New Castle, DE) was added to the slurry using a ratio of 2 ml of 15 wt% liquid Nafion to 20 ml of isopropanol. The CCM was dried in a vacuum oven at 50°C for 30 minutes. Both commercial catalyst and platinum supported on MWCNTs catalyst were made into slurry and CCM using the same procedure.

The CCMs and gas diffusion layers (Hollingsworth and Vose) were assembled in a single test cell (Fuel Cell Technologies, Albuquerque, NM, USA) by sandwiching them together with silicone-coated fabric (CF1007, Saint-Gobain Performance Plastics) to provide gas sealing. The cells were closed and tightened to a uniform torque of 40 lb-in. Fuel cell performance was tested using galvanostatic polarization with Greenlight Test Station (G50 Fuel cell system, Hydrogenics, Vancouver, Canada). The cells were purged with nitrogen and tested at 70°C with H<sub>2</sub>/O<sub>2</sub>. Hydrogen gas flowed over the anode at a rate of 0.2 SCCM and oxygen flowed over the cathode at a rate of 0.4 SCCM both at 100% relative humidity. The CLs were not tested in air since the oxygen system better portrays the potential and performance of the CLs.

### **3.4. Results and Discussion**

The particle size and distribution of platinum on multi-walled carbon nanotubes was drastically improved by controlling the equipment and parameters used to deposit the platinum on the MWCNTs from Process 1 (prior work<sup>21</sup>) to Process 2 (improved

procedure, introduced here). In the prior work<sup>12</sup>, platinum nanoparticle size ranged from 8-10 nm while the platinum nanoparticle size was reduced in the improved procedure and ranged from 2-4 nm. Figure 3.1 shows a TEM image of Process 1 compared to the improved Process 2 shown in Figure 3.2. Prior research, in this work, utilizing variations of this procedure produced inferior platinum distribution and particle size (see Figure 3.1<sup>21</sup>). These procedures also used different equipment and processing parameters. The results of this improved process show that the methodology used here to support platinum on MWCNTs is highly dependent upon the equipment setup and processing parameters. The fuel cell testing results show that using MWCNTs as a catalyst support increase the efficient utilization of the platinum catalyst. Additionally, the distribution and homogeneity shown here is better than other reports in the literature<sup>25-33</sup>.

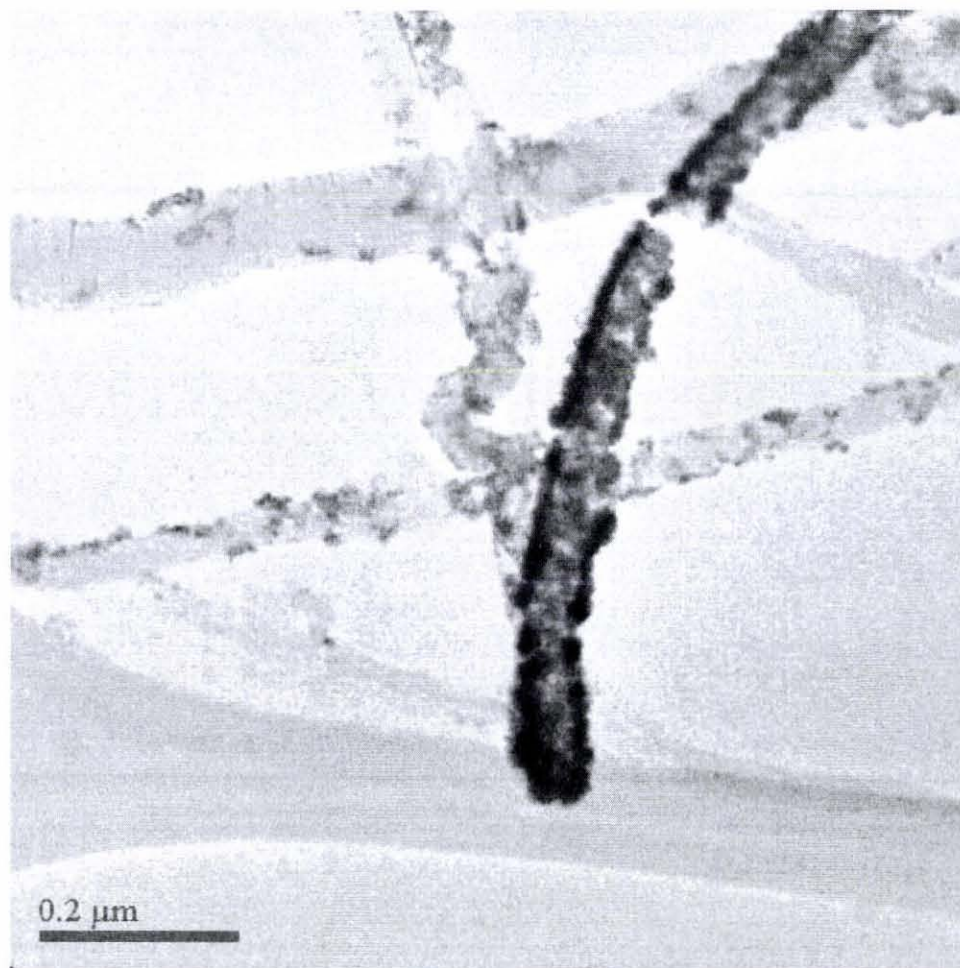
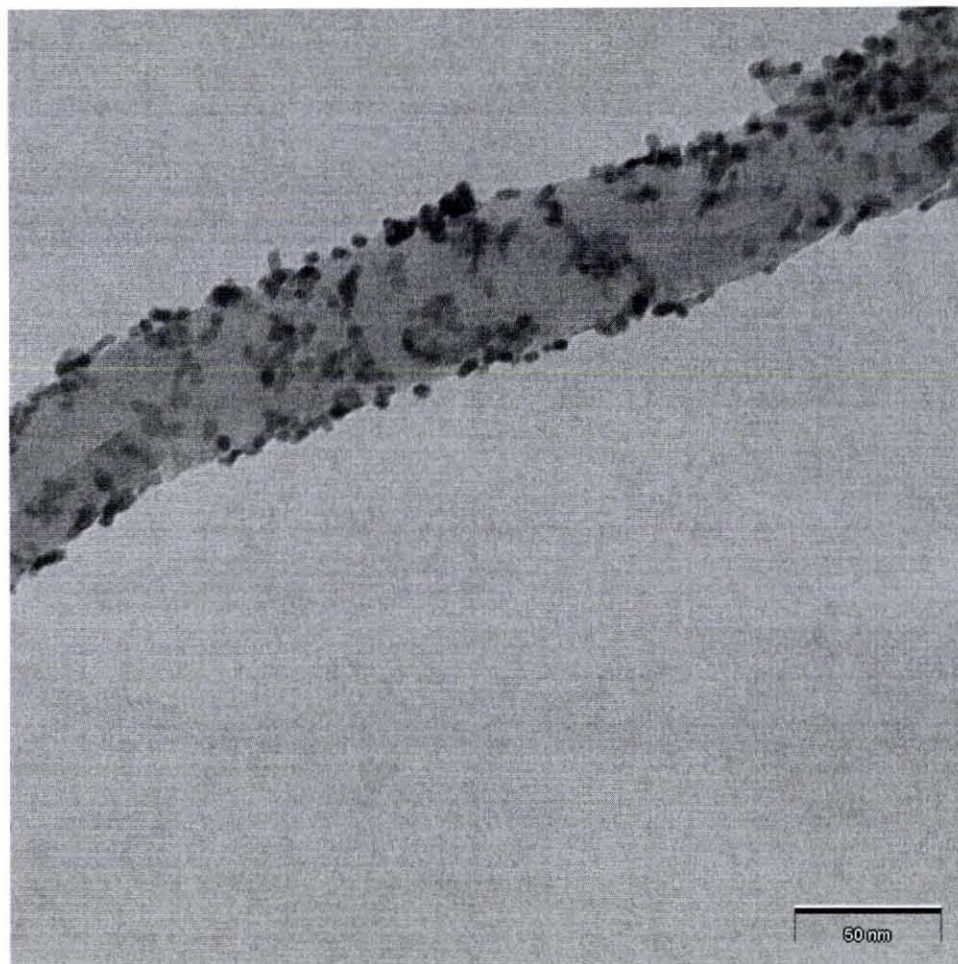


Figure 3.1. TEM micrograph showing the platinum nanoparticles distribution on MWCNTs from prior work using Process 1<sup>21</sup>.



**Figure 3.2. TEM micrograph showing the platinum nanoparticle distribution on MWCNTs from current work using refined procedures via Process 2**

All MWCNTs used in the experimentation appeared to be homogenous and were fabricated using the same chemical vapor deposition setup and parameters. The MWCNTs were taken from the silicon substrates and combined in one container. Since all MWCNTs were fabricated using identical processing conditions and parameters, all should have similar structural and defect properties. Thus, it is believed that the differences seen in the platinum nanoparticle distribution and particle size can be related to the process by which the platinum nanoparticles are deposited onto MWCNTs. While the defect structures of the MWCNTs used in these procedures were not analyzed here, it

should be mentioned that much work has been conducted to functionalize MWCNTs by creating defect sites for the deposition of nanoparticles<sup>25-33</sup>. These functionalized MWCNTs have been used by others for platinum nanoparticles deposition and claimed that these structures help with platinum nanoparticles dispersion and particle size on MWCNTs<sup>25-33</sup>. It is worth noting that no steps (including the use of concentrated acids) were used in this new procedure to create defect sites on the carbon nanotubes.

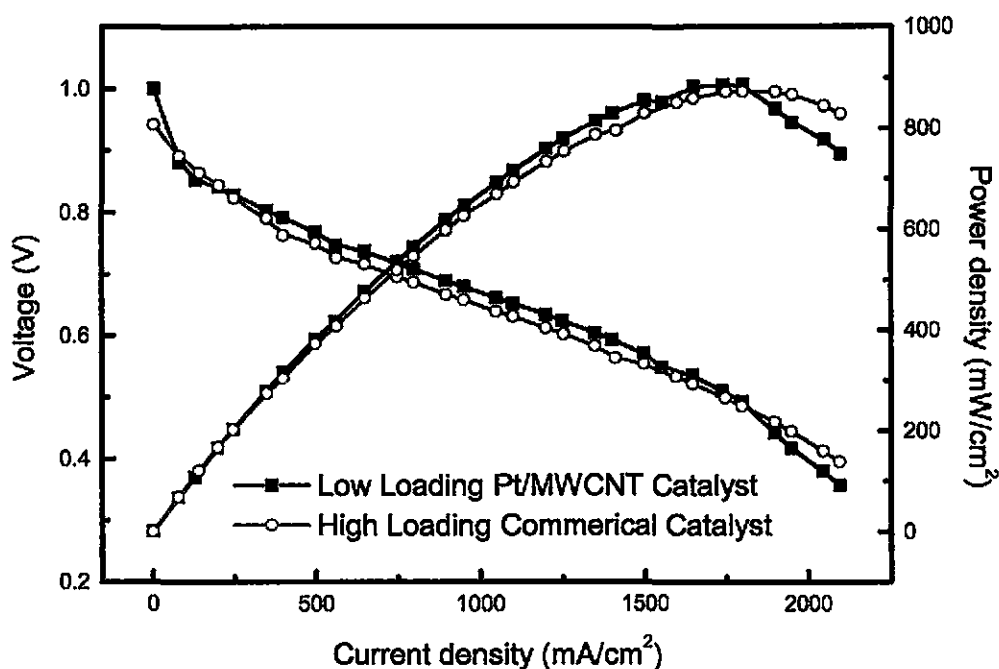


Figure 3.3. Galvanostatic polarization and power density plots for testing Pt/MWCNT catalyst.

Testing the developed catalyst layer at the anode in a H<sub>2</sub>/O<sub>2</sub> proton exchange membrane fuel cell shows a very good cell performance. The results from galvanostatic polarization testing of Pt/MWCNT fuel cell catalyst are shown in Figure 3.3. The high loading

commercial catalyst layer cell contained twice the platinum loading per area compared to the 50 wt% Pt/MWCNT fuel cell and achieved a somewhat lower performance result (see Figure 3.3). The commercial catalyst cell contained 2.5 mg of Pt/cm<sup>2</sup> on the electrode surface while the low loading Pt/MWCNT catalyst contained 0.65 mg of Pt/cm<sup>2</sup> on the electrode surface. This equates to a 74% decrease in platinum loading on the membrane with about 2% performance enhancement. The current that was obtained was up to 2 amps per cm<sup>2</sup> (see Figure 3.3). Future work should focus on the mechanics of platinum nanoparticles deposition on the multi-walled carbon nanotube.

### **3.5. Conclusions**

It is feasible to use MWCNTs as a platinum catalyst support for proton exchange membrane fuel cells. It has been shown that the equipment and process used to deposit the platinum solution on the carbon nanotubes determines the platinum nanoparticles particle size and distribution on the carbon nanotube. These results go against other theories that the distribution is related to the types of chemicals used or the defect structure of the carbon nanotube.

## **CHAPTER 4**

# **NOVEL USE OF PLATINUM NANO-WIRES AS A CATALYST FOR PROTON EXCHANGE MEMBRANE FUEL CELLS**

### **4.1. Overview**

The use of platinum nano-wires as a catalyst is a novel concept that has never been attempted before in the literature. Nano-structured wires with optimized length would provide the 3-phase contact needed at the membrane, catalyst, and reactants<sup>20</sup>. Furthermore, the inherent structure of the nanowires provides the porosity needed to promote reactant gas exchange. When combining the porous nature of the platinum nanowires with their high electrical conductivity, they are expected to work much better than platinum nanoparticles in PEMFCs although they have lower surface area to volume ratios when compared to platinum nanoparticles supported on carbon or carbon nanotubes. The fuel cell testing of the platinum nanowires, using hydrogen and oxygen at ambient pressure, shows promise for this concept.

### **4.2. Introduction**

Proton exchange membrane fuel cells (PEMFCs) are emerging in the market as devices that provide power for stationary and portable power devices. The utilization and effective use of expensive platinum catalysts is preventing them from being fully commercialized. Advancements in supporting platinum on various carbon supports have

made the use of platinum black cost prohibitive and inefficient<sup>1</sup>. The advents of nanotechnology have made it possible to design and fabricate platinum nanowires with features that are beneficial to the performance of PEMFCs.

## **4.3. Experimental**

### ***4.3.1. Experimental Overview***

Membrane electrode assemblies (MEAs) were constructed with platinum nanowires (received from Rensselaer Polytechnic Institute) hot pressed to the anode side of a Nafion® NRE-211 membrane (Ion Power, Inc. New Castle, DE) and then after the hot-pressing technique, commercially available catalyst was made into a slurry and applied to the cathode side of the membrane using micro-spray technique. The details of each technique are discussed in the subsequent sections.

### ***4.3.2. Procedure for Hot Pressing***

The hot press plates were preheated to 155 °C. The silicon wafer substrate (1 in<sup>2</sup>) with platinum nano-wires was centered on a large PTFE coated cloth with a 3X3” section of Nafion® NRE-211 centered over platinum nano-wires. Another PTFE coated cloth was placed over the membrane to prevent the membrane from sticking to the plates. The plates were compressed to 120 lbs/cm<sup>2</sup> for five minutes to ensure the transfer of the nano-wires from the substrate to the membrane. The components were removed from the hot

press and cooled at room temperature on the lab bench while compressed with 15 kg of lead weights to prevent warping. Once cooled, the MEA was carefully peeled from the silicon wafer substrate. An active area of  $2 \text{ cm}^2$  was fabricated based on the coverage of the platinum nanowires.

#### ***4.3.3. Procedure for Micro-Spray Technique***

The cathode side was micro-sprayed with a catalyst slurry prepared by conditioning commercially available platinum 50wt% supported on Vulcan XC-72 (TEC10V50E Tanaka, Indianapolis, IN ) over flowing nitrogen for 30 min to prevent ignition, then slowly adding 10 ml of isopropanol and 1.6 ml of 15 wt% Nafion® solution (Ion Power Inc, New Castle, DE). The mixture was sonicated to improve homogeneity for 10 min, and then magnetically stirred for 60 min. The MEA was dried in a vacuum oven at  $50^\circ\text{C}$  for 30 minutes.

#### ***4.3.4. Fuel Cell Testing***

The completed MEA was sandwiched into a test cell (Fuel Cell Technologies, Albuquerque, NM, USA) using Hollingsworth and Vose carbon paper for the gas diffusion layers and silicone coated fabric (CF1007, Saint-Gobain Performance Plastics) to provide gas sealing. The cells were closed and tightened to a uniform torque of 40 lb-in. The cells performance was tested using galvanostatic polarization with Greenlight Test Station (G50 Fuel cell system, Hydrogenics, Vancouver, Canada). The cells were purged with nitrogen and tested at  $70^\circ\text{C}$  with  $\text{H}_2/\text{O}_2$ . Hydrogen gas flowed over the

anode at a rate of 0.2 SCCM and oxygen flowed over the cathode at a rate of 0.4 SCCM both at 100% relative humidity. Again, The CLs were not tested in air since the oxygen system better portrays the potential and performance of the CLs.

#### **4.4. Results and Discussion**

The platinum loading using the nanowires was determined to be  $0.32 \text{ mg/cm}^2$  based on calculations from the SEM images of the as-grown platinum nanowires on the silicon substrate shown in Figures 4.1 and 4.2, which a top view perspective of the as-received platinum nanowires on the silicon substrate and a side view of the as-received platinum nanowires, respectively. The height of the platinum nano-wires on the silicon substrate is 300 nm (measured in Figure 4.2) with diameters of the platinum nanowires ranging from 10 to 50 nm. The wires cover approximately 50% of the area. This catalyst loading falls well within allowable limits.

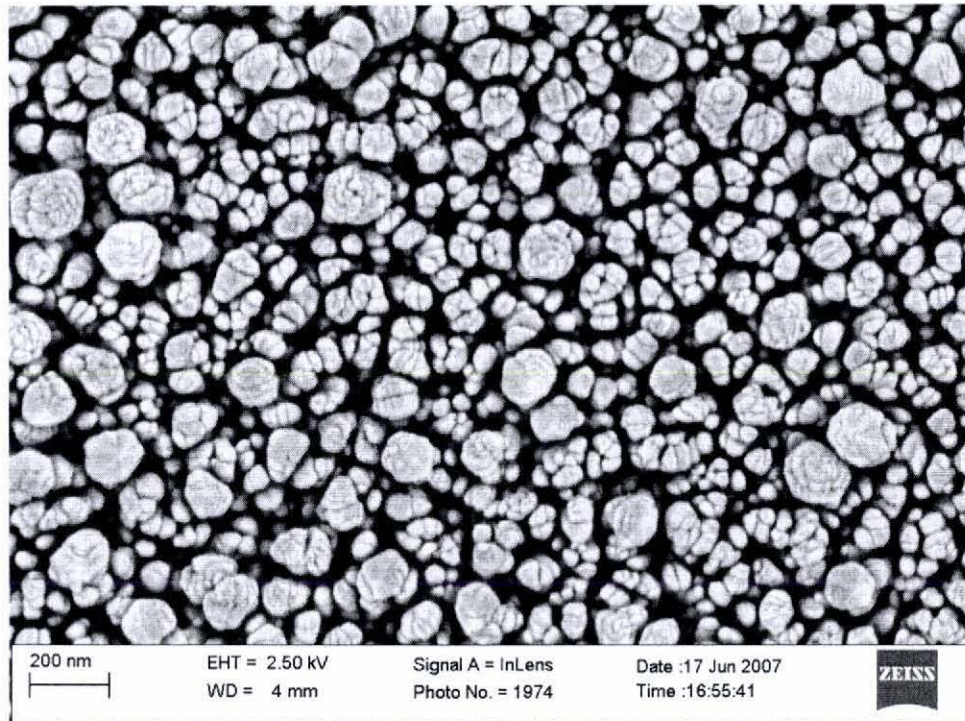
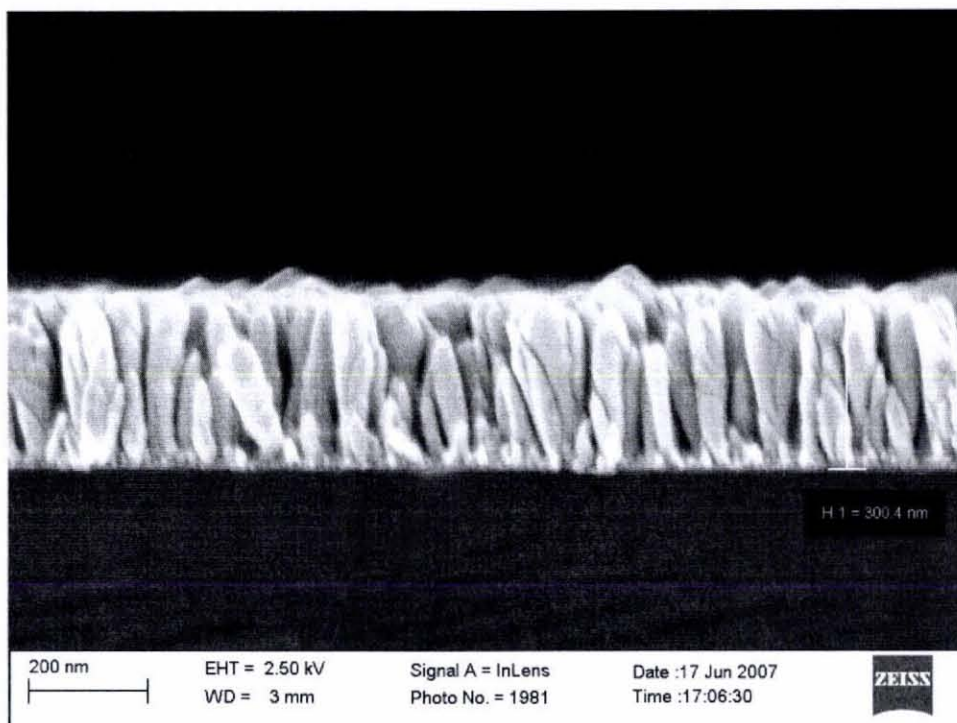
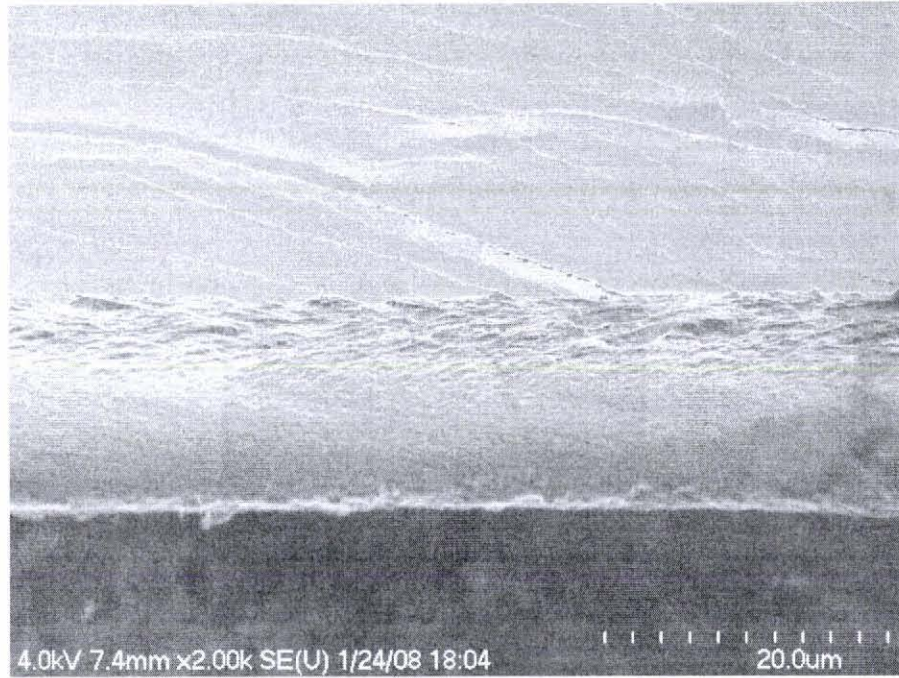


Figure 4.1. SEM image of the as-grown platinum nanowires on silicon substrate showing the porous nature of this nanostructure from the top view.



**Figure 4.2. SEM image of the as-grown platinum nanowires on silicon substrate showing the porous nature of this nanostructure from the side view.**

The hot pressing procedure developed in this project to transfer the as-received platinum nanowires from the silicon substrate to the Nafion® NRE-211 membrane is very effective and well designed as 100% of the platinum nanowires were uniformly transferred to the membrane (i.e., successfully transferred a vertically aligned forest of platinum nanowires). The SEM micrograph taken at a 45° stage tilt in Figure 4.3 shows a cross-sectional view of the platinum nanowires hot-pressed to the Nafion® NRE-211 membrane. Since the nanowires are so small, they are not easily identified in Figure 4.3 but can be seen in Figure 4.4 which is a higher magnification SEM. Figure 4.4 is interesting because the surface of the nanowires has a smooth surface instead of the expected porous structure shown in Figure 4.1.



**Figure 4.3. SEM cross-sectional view of platinum nanowires on Nafion® NRE-211 taken at a 45° stage tilt showing the lead film covering the nanowires and the cracks in the metallic film.**



**Figure 4.4. SEM cross-sectional view of platinum nanowires on Nafion® NRE-211 taken at a 45° stage tilt showing the aligned structure of the nanowires.**

Figure 4.5 shows the results from the galvanostatic polarization testing comparing a fuel cell made with the platinum nanowires on the anode to a fuel cell made with commercially available catalyst. Notice that the fuel cell constructed with the platinum nanowires on the anode barely performs compared to the fuel cell constructed with commercially available catalyst.

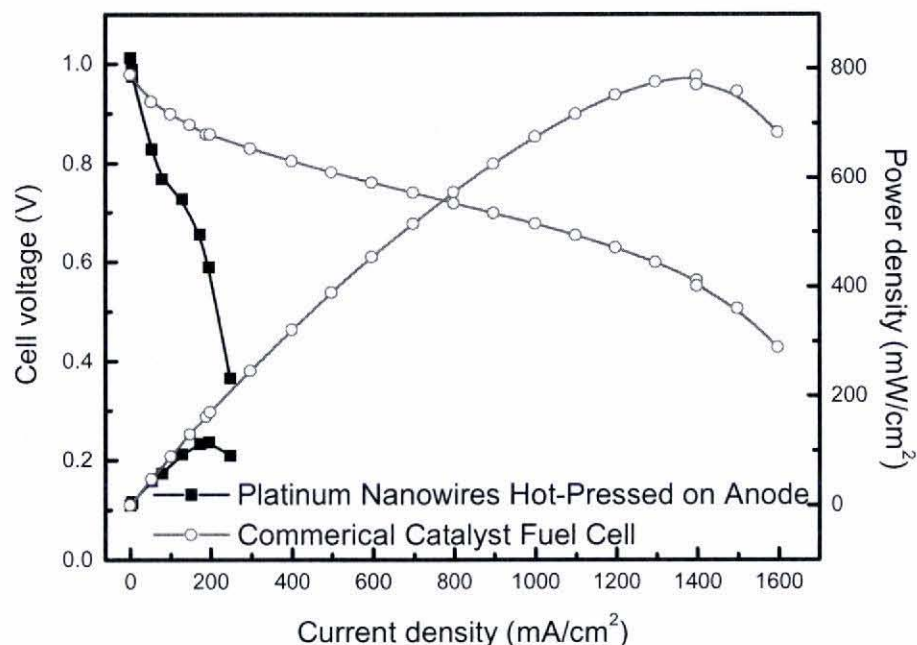


**Figure 4.5. Fuel cell voltage and power density measured by galvanostatic polarization comparing a cell made with the platinum nanowires on the anode to a fuel cell made with commercially available catalyst.**

The SEM in Figure 4.6 reveals a thin metallic layer at the base of the platinum nanowire nanoforest. This thin metallic lead layer created a barrier such that the reactant gases could not reach all available catalyst sites. Re-inspection of Figure 4.3 show small cracks in the metallic layer. It should be noted that the surface view in Figure 4.3 does not show the expected porous nature of the as-grown nano-wires because the thin metallic layer deposited at the base of the platinum nanowire nanoforest was also transferred during the hot-pressing procedure. Anodic reactions only occurred where there were cracks in the surface of the metallic layer or at the edges of the metallic layer. This metallic layer explains why the fuel cell performance is low (see Figure 4.5). The element analysis in

Figure 4.7 taken from the SEM shown in Figure 4.4 shows the presence of platinum from the platinum nanowires and the presence of lead, which is most likely used in the manufacture of the as-received platinum nanowires and is the metallic layer that prohibited the flow of gases for the anodic reaction.

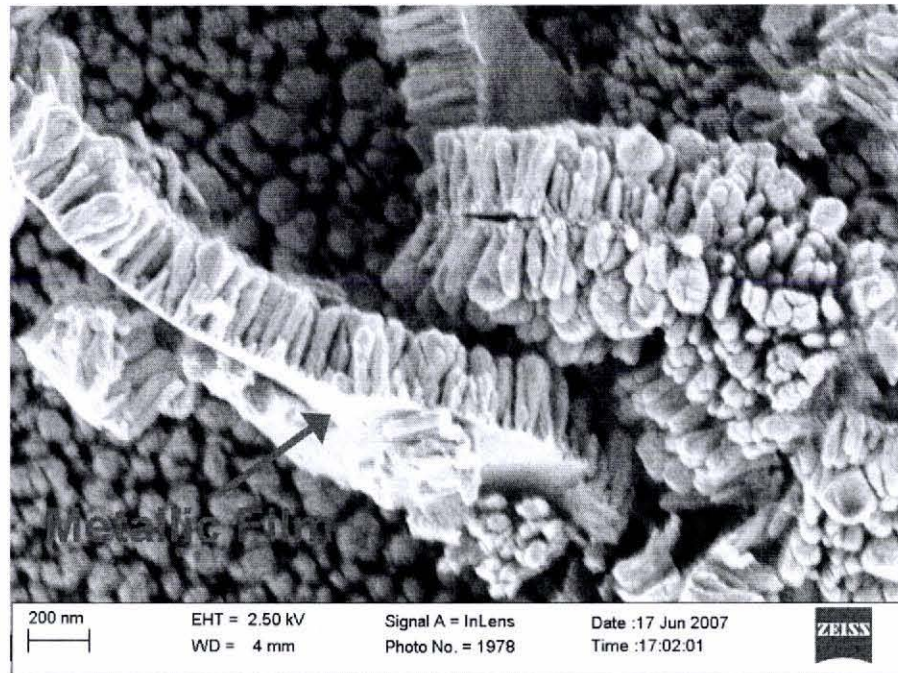


**Figure 4.6. SEM of as-received platinum nanowires detached from the substrate showing a thin metallic layer at the base of the platinum nanowire forest.**

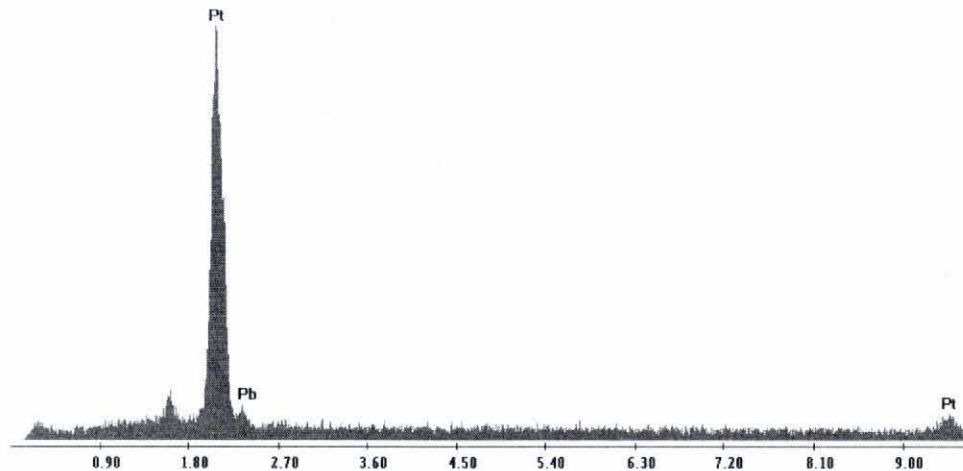


Figure 4.7. Elemental analysis showing the presence of platinum and lead in the SEM images.

## 4.5. Conclusions

The results of the fuel cell testing show that platinum nano-wires can be used as a catalyst layer for PEMFCs. The hot-pressing procedure developed in this work is an excellent method to transfer vertically aligned platinum nanowires to Nafion®. Furthermore, fabricating catalyst layers with vertically aligned platinum nanowires creates an ideal porous structure and provides uniform coverage over the entire active catalyst layer. Future work needs to be conducted to remove the metallic layer from the platinum nanowires so that the full potential of this concept can be proven in fuel cell testing.

# CHAPTER 5

## GENERAL CONCLUSIONS

The in-situ modified carbon papers with the direct growth of carbon nanotube nanoforest shows excellent performance over a wide range of humidity conditions, including lower humidity when compared to plain as-received teflonized carbon papers. The performance of fuel cells that operate with atmospheric air, unstable humidity conditions, or with simplified humidification systems could be significantly enhanced using the in-situ gas diffusion layer developed here. To fully realize the potentials of the gas diffusion layer developed here, a long-term durability test should be conducted to ensure continuous operation.

It is feasible to use MWCNTs as a platinum catalyst support for proton exchange membrane fuel cells. It has been shown that the equipment and process used to deposit the platinum solution on the carbon nanotubes determines the platinum nanoparticle particle size and distribution on the carbon nanotube. These results go against other theories that the distribution is related to the types of chemicals used or the defect structure of the carbon nanotube.

The results of the fuel cell testing show that platinum nano-wires can be used as a catalyst layer for PEMFCs. The hot-pressing procedure developed in this work is an excellent method to transfer vertically aligned platinum nanowires to Nafion®. Furthermore, fabricating catalyst layers with vertically aligned platinum nanowires creates an ideal

porous structure and provides uniform coverage over the entire active catalyst layer. Future work needs to be conducted to remove the metallic layer from the platinum nanowires so that the full potential of this concept can be proven in fuel cell testing.

As the development of fuel cell technology continues and as the commercialization of these products grow, the scientific community and industry will need to take new approaches to improve upon existing technology. It has been demonstrated in the main works discussed in this thesis that there are numerous useful nanotechnology applications that can be applied to fuel cells.

## **APPENDIX**

# **POLARIZATION CURVES FOR THE DEVELOPMENT OF IN-SITU MODIFIED CARBON PAPERS WITH MULTI-WALLED CARBON NANOTUBES USED AS GAS DIFFUSION LAYERS FOR PROTON EXCHANGE MEMBRANE FUEL CELLS**

The calculations made in the appendix for peak power density improvement and voltage improvement at peak power density may contain up to +/- 5% experimental error.

**A.1. The following figures give the polarization plots for fuel cell testing in hydrogen and oxygen at the 70 °C and various relative humidity.**

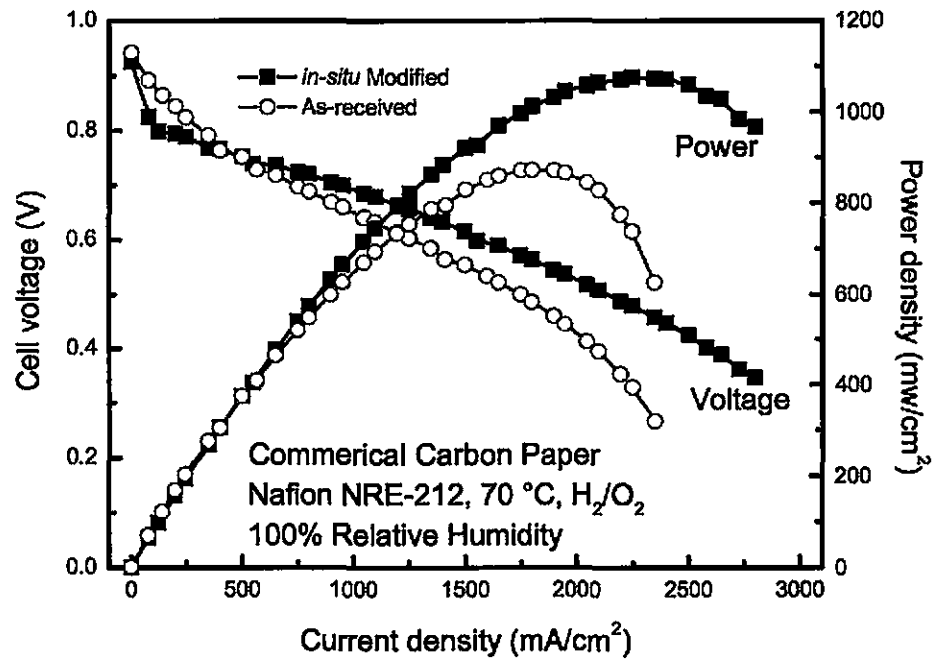


**Figure A.1.1. 100% RH, 24% peak power improvement, -1% voltage improvement at peak power density.**

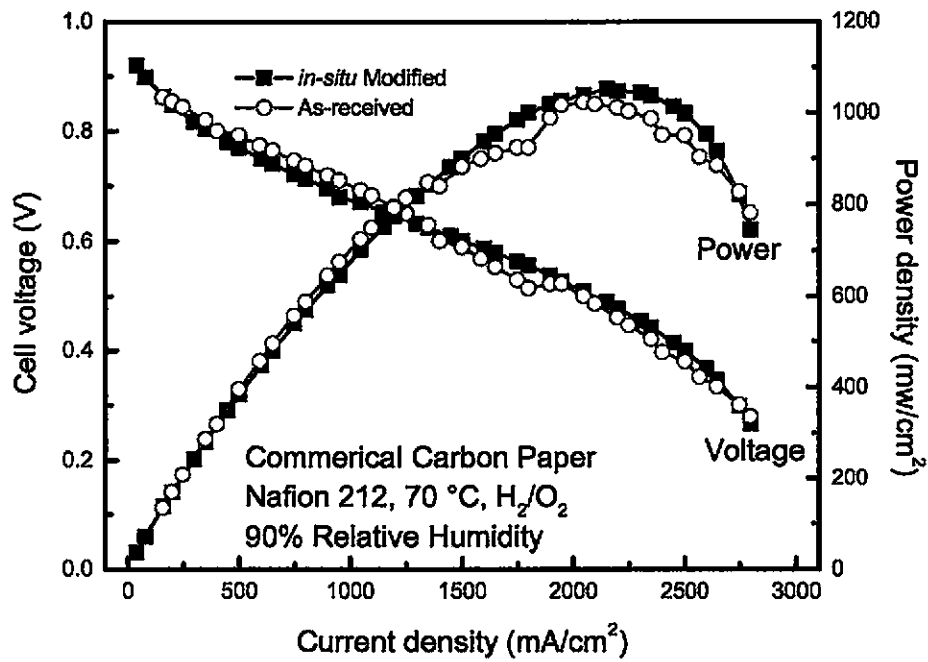


**Figure A.1.2. 90% RH, 3% peak power improvement, -2% voltage improvement at peak power density.**

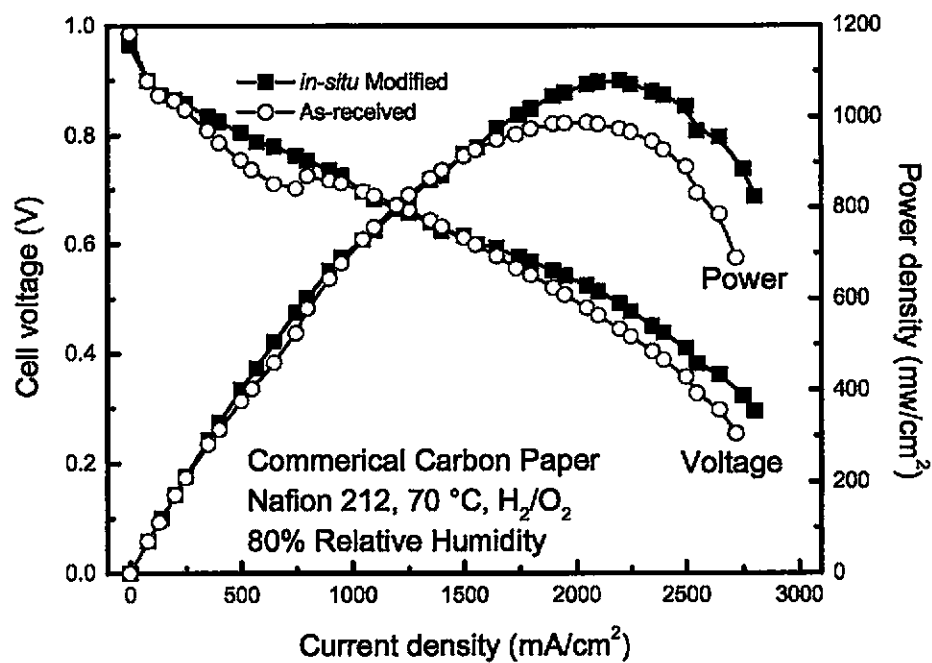


**Figure A.1.3. 80% RH, 9% peak power improvement, 2% voltage improvement at peak power density.**

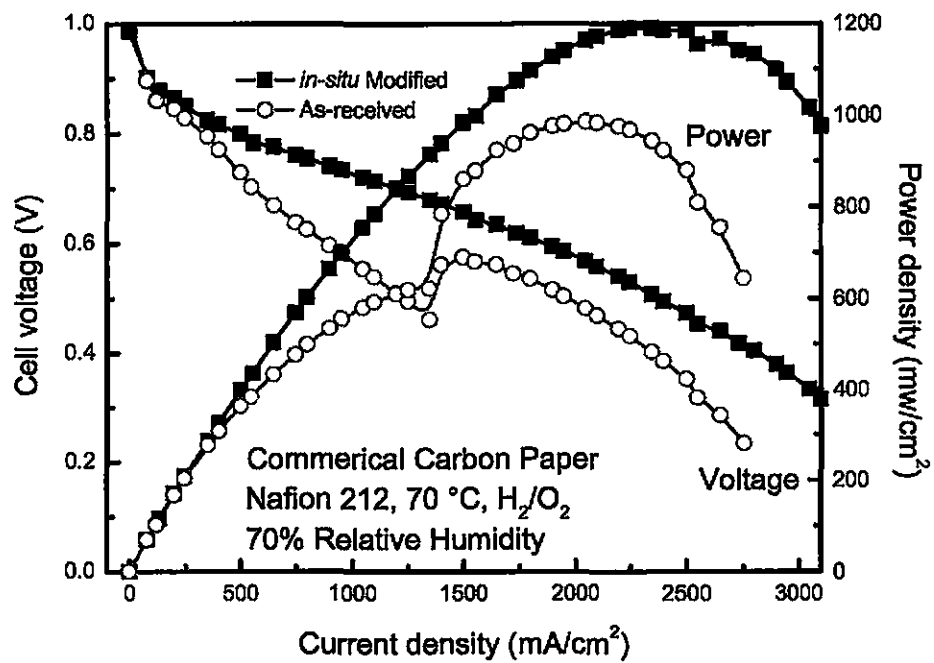


**Figure A.1.4. 70% RH, 21% peak power improvement, 5% voltage improvement at peak power density.**

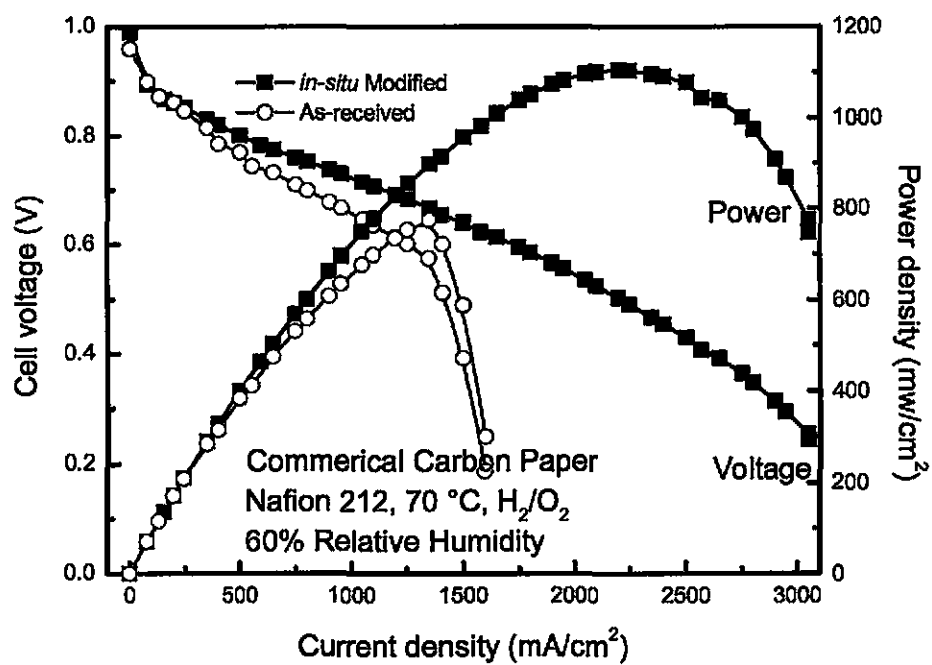


**Figure A.1.5. 60% RH, 43% peak power improvement, -12% voltage improvement at peak power density.**

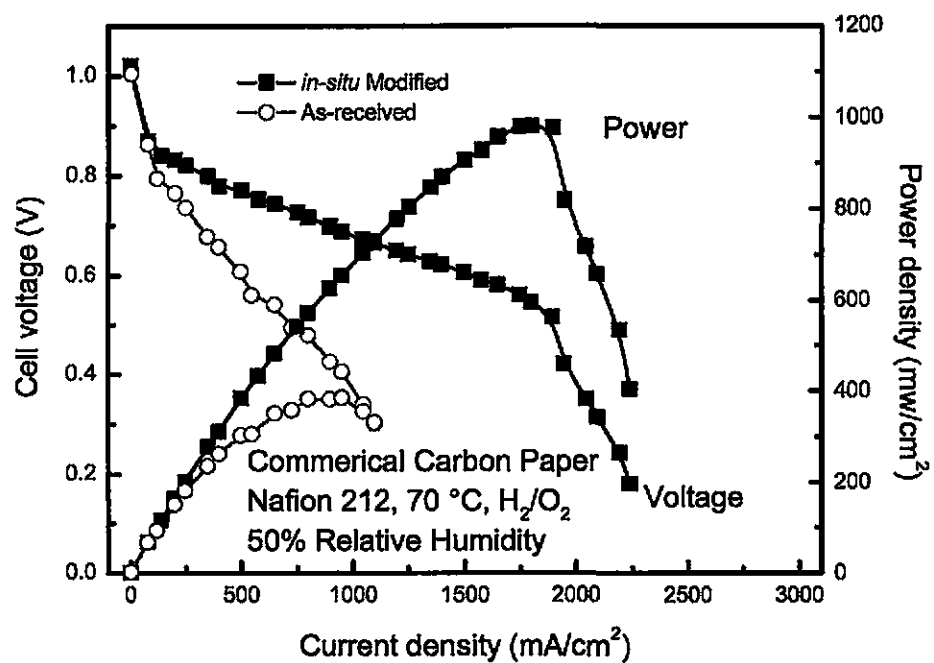


**Figure A.1.6. 50% RH, 155% peak power improvement, 14% voltage improvement at peak power density.**

**A.2. The following figures give the polarization plots for fuel cell testing in hydrogen and air at 70°C and various relative humidity.**

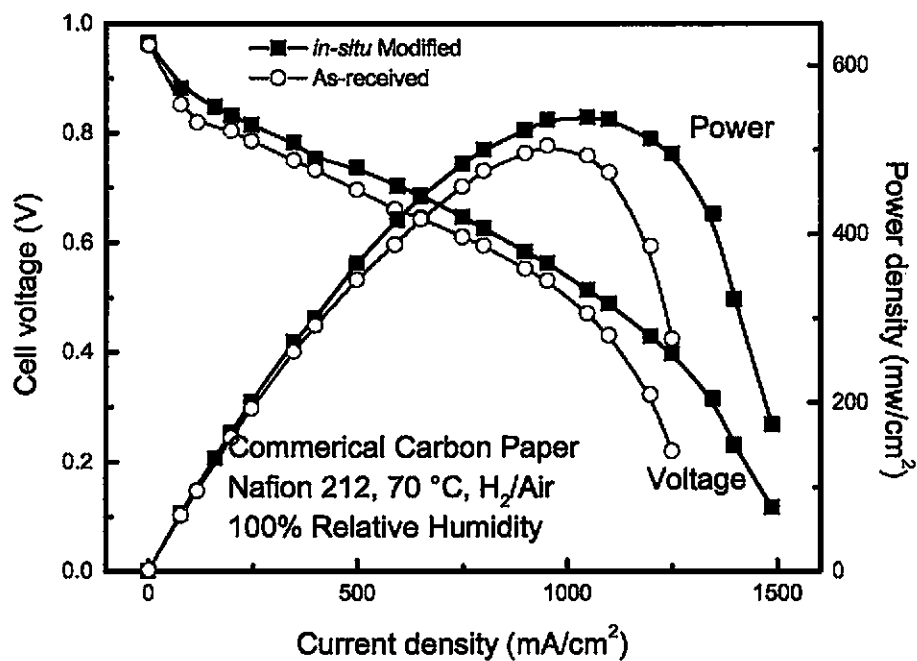


**Figure A.2.1. 100% RH, 6% peak power improvement, -3% voltage improvement at peak power density.**

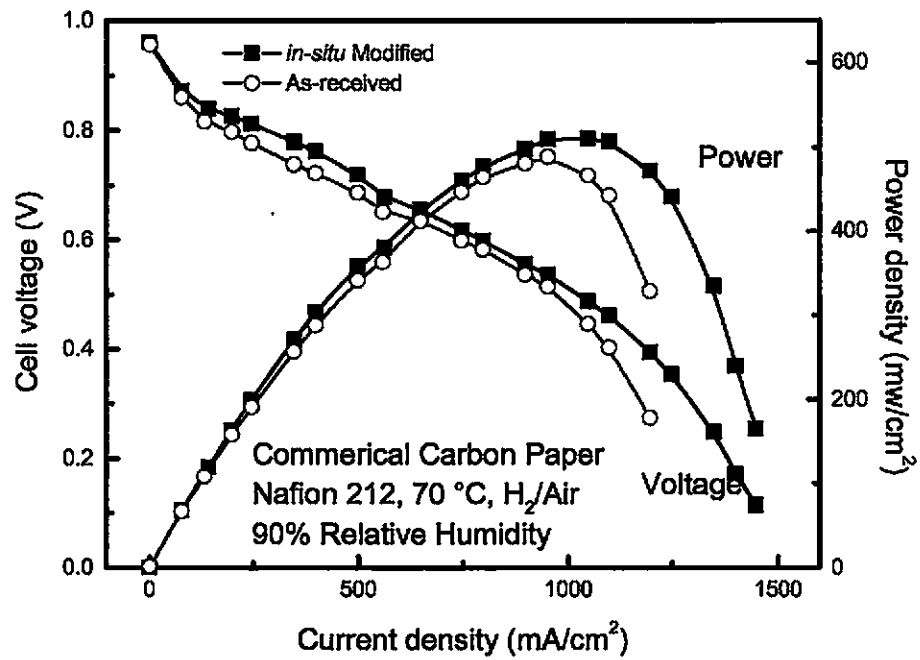


**Figure A.2.2. 90% RH, 4% peak power improvement, -5% voltage improvement at peak power density.**

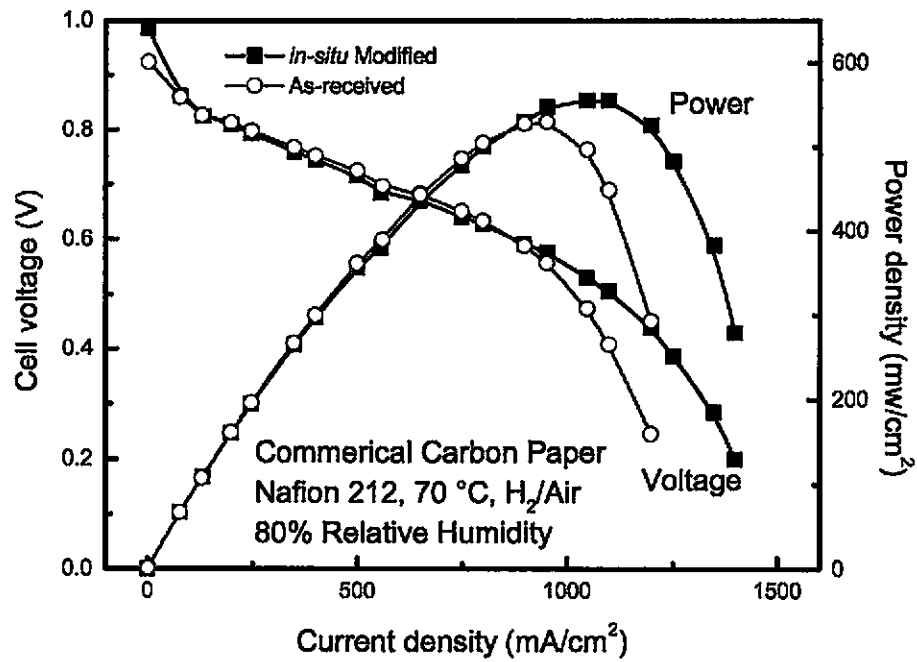


**Figure A.2.3. 80% RH, 5% peak power improvement, -5% voltage improvement at peak power density.**

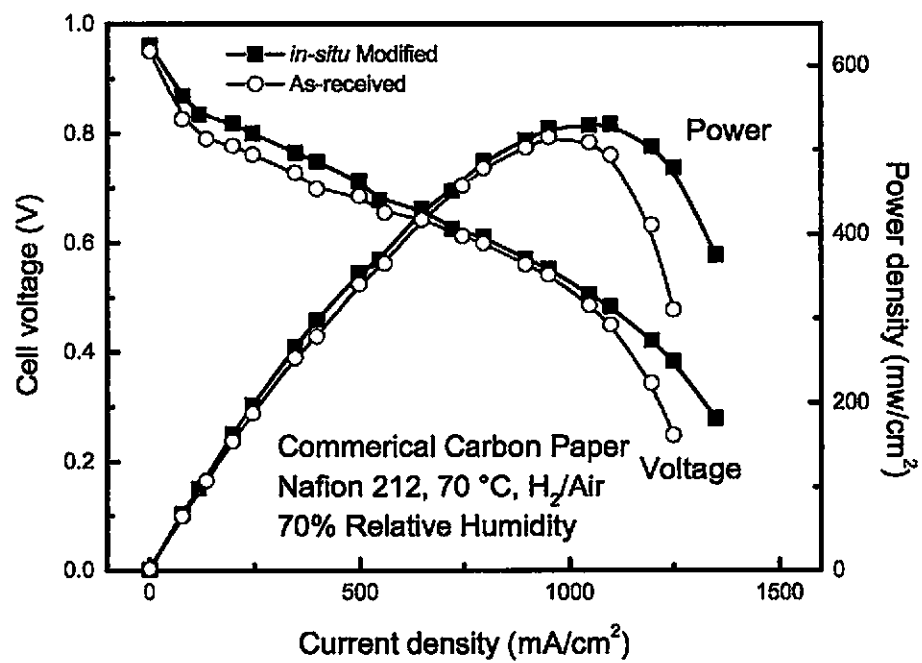


**Figure A.2.4. 70% RH, 3% peak power improvement, -11% voltage improvement at peak power density.**

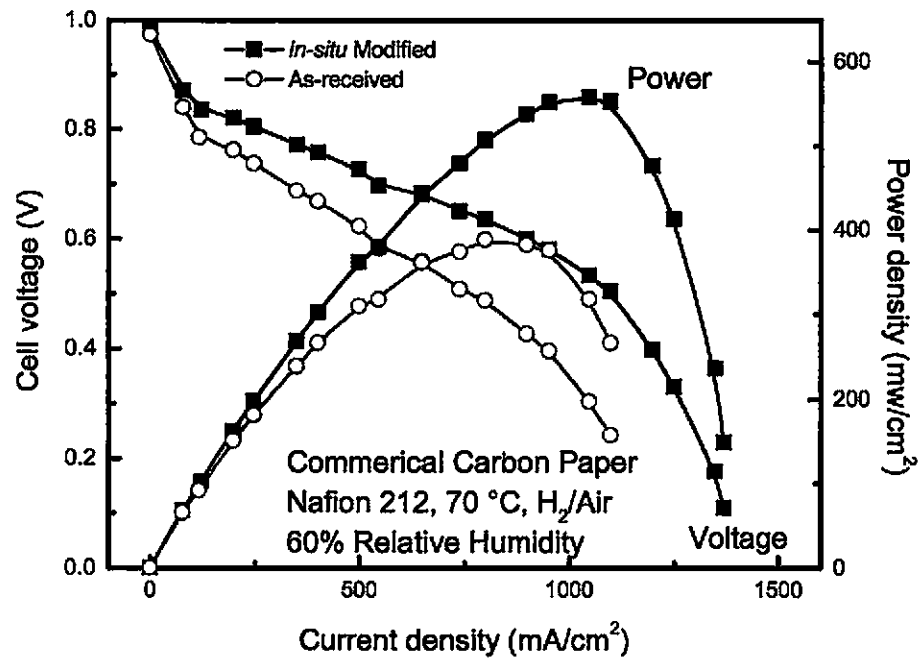


**Figure A.2.5. 60% RH, 43% peak power improvement, 9% voltage improvement at peak power density.**

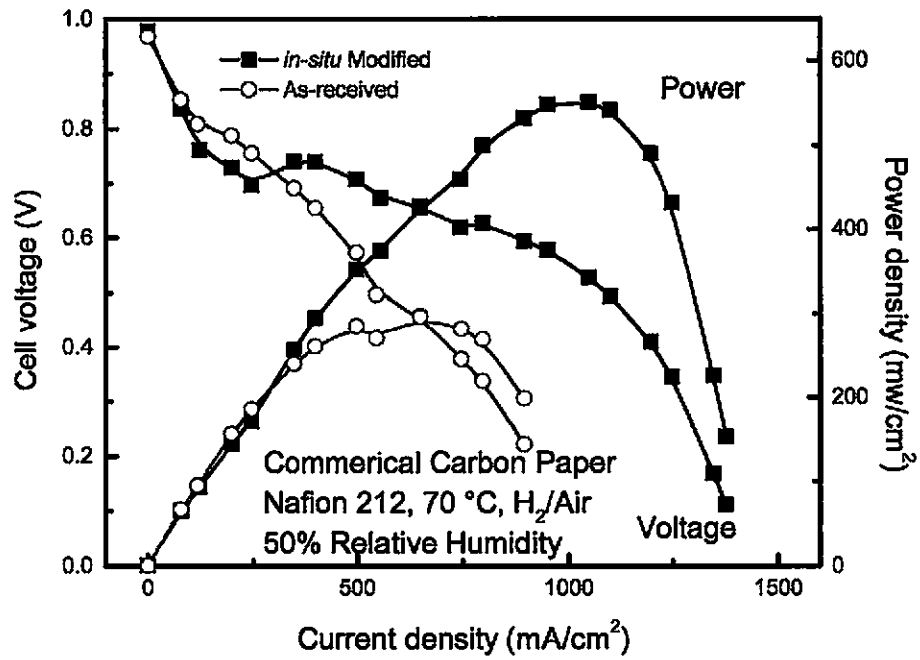


**Figure A.2.6. 50% RH, 86% peak power improvement, 15% voltage improvement at peak power density.**

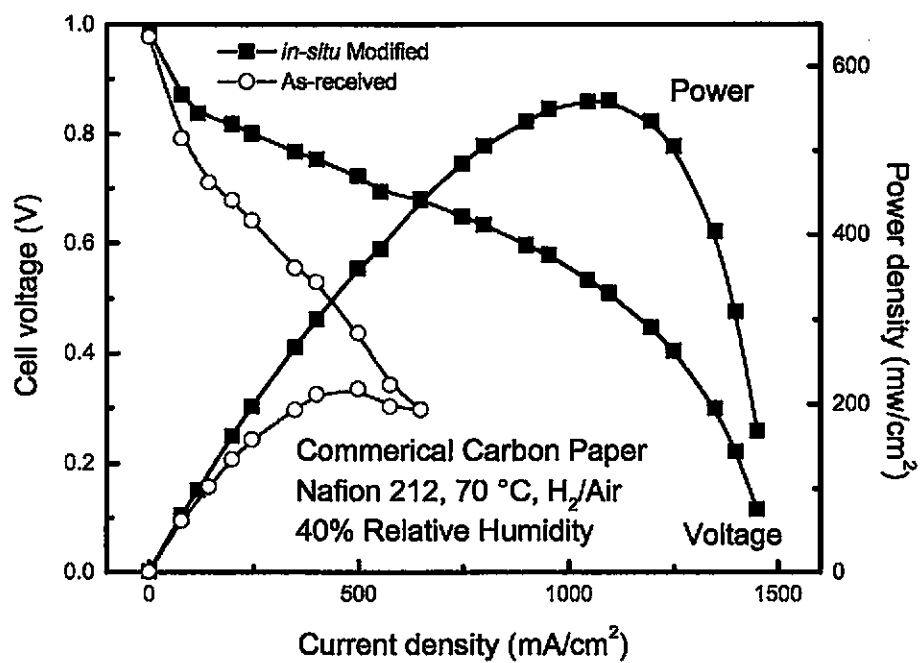


**Figure A.2.7. 40% RH, 157% peak power improvement, 16% voltage improvement at peak power density.**

# REFERENCES

- 
- <sup>1</sup> Laramie, J., and Dicks, A. Fuel cell systems explained. 2<sup>nd</sup> ed. New York. Wiley. (2003).
- <sup>2</sup> Zawodzinski, T., Springer, T., Davey, J., Jestel, R., Lopez, C., Valerio, J., and Gottesfeld, S. A comparative study of water uptake by transport through ionomeric fuel cell membranes. *Journal of the Electrochemical Society*. **140**. 1981-1985. (1993).
- <sup>3</sup> Bernardi, D. Water-balance calculations for solid-polymer-electrolyte fuel cells. *Journal of the Electrochemical Society*. **137**. 3344-3350. (1990).
- <sup>4</sup> Chiang, M., and Chu, H. Effects of temperature and humidification levels on the performance of a proton exchange membrane fuel cell. *Journal of Power and Energy*. **220**. 435-448. (2006).
- <sup>5</sup> Ren, X., and Gottesfeld, S. Electro-osmotic drag of water in poly(perfluorosulfonic acid) membranes. *Journal of the Electrochemical Society*. **148**. A87-A93. (2001).
- <sup>6</sup> Chen, D., Li, W., and Peng, H. An experimental study and model validation of a membrane humidifier for PEM fuel cell humidification control. *Journal of Power Sources*. **180**. 461-467. (2008).
- <sup>7</sup> Whittingham, M., Savinell, R., and Zawodzinski, T. *Chemical Reviews*. **104**. 4243-4244. (2004).
- <sup>8</sup> Service, R. Shrinking fuel cells promise power in your pocket, *Science*, **296**, 1222-1224 (2002).
- <sup>9</sup> Zawodzinski, T., Derouin, C., Radzinski, S., Sherman, R., Smith, V., and Springer, T., and Gottesfeld, S., Water uptake by and transport through Nafion 117 membranes. *Journal of the Electrochemical Society*. **140**. 1041-1047 (1993).
- <sup>10</sup> Buchi, F., and Srinivasan, S. Operating proton exchange membrane fuel cells without external humidification of the reactant gases. Fundamental aspects. *Journal of the Electrochemical Society*. **144**. 2767-2772 (1997).
- <sup>11</sup> Dicks, A. The role of carbon in fuel cells. *Journal of Power Sources*. **156**. 128-141. (2006).
- <sup>12</sup> Kannan, A., Veedu, P., Munukulta, L., and Ghasemi-Nejhad, M. N. Nanostructured gas diffusion and catalyst layers for proton exchange membrane fuel cells. *Electrochemical and Solid State Letters*. **10**. B47-B50 (2007).
- <sup>13</sup> Kannan, A., Cindrella, L., and Munukulta, L. Functionally graded nano-porous gas diffusion layer for proton exchange membrane fuel cells under low relative humidity conditions. *Electrochimica Acta*. **53**. 2416-2422. (2008).
- <sup>14</sup> Chen-Yang, Y., Hung, T., Huang, J., and Yang, F. Novel single-layer gas diffusion layer based on PTFE/carbon black composite for proton exchange membrane fuel cell. *Journal of Power Sources*. **173**. 183-188. (2007).
- <sup>15</sup> Park, G., Sohn, Y., Yim, S., Yang, T., Yoon, Y., Lee, W., Eguchi, K., and Kim, C. Adoption of nano-materials for the micro-layer in gas diffusion layers of PEMFCs. *Journal of Power Sources*. **163**. 113-118. (2006).

- 
- <sup>16</sup> Liu, C., and Cheng, H. Carbon nanotubes for clean energy applications. *J. of Phys. D: appl. Phys.* **38**. R231-R252. (2005).
- <sup>17</sup> Li, H., Lu, W., Li, J., Bai, X., and Gu, C. Multichannel Ballistic Transport in Multiwall carbon nanotubes. *Physical Review Letters*. **95**. 086601. (2005).
- <sup>18</sup> Lau, K., Bico, J., Teo, K., Chhowalla, M., Amaratunga, G., Milne, W., McKinley, G., and Gleason, K. Superhydrophobic Carbon Nanotube Forests. *Nano Lett.*, **3**, 1701-1705 (2003).
- <sup>19</sup> Brukh, R., and Mitra, S. Kinetics of carbon nanotube oxidation. *Journal of Materials Chemistry.*, **17**, 619-623 (2006).
- <sup>20</sup> Lee, S., Mukerjee, S., McBreen, J., Rho, Y. Kho, Y., and Lee, T. Effects of Nafion impregnation on performances of PEMFC electrodes. *Electrochemical Acta*. **43**. 3693-3701 (1998).
- <sup>21</sup> Kannan, A., Stuckey, P., Ghasemi-Nejhad, M. N. Platinum supported on carbon nanotubes for proton exchange membrane fuel cells. *2007 Fuel Cell Seminar and Exposition*. San Antonio, TX. October 2007.
- <sup>22</sup> Brukh, R., and Mitra, S. Kinetics of carbon nanotube oxidation. *Journal of Materials Chemistry*. **17**, 619-623 (2006).
- <sup>23</sup> Rajalakshmi, N., Ryu, H., Shaijumon, M., Ramaprabhu, S. Performance of polymer electrolyte membrane fuel cells with carbon nanotubes as oxygen reduction catalyst support material. *Journal of Power Sources*. **140**. 250-257 (2005).
- <sup>24</sup> Wang, M., Woo, K., Kim, D. Preparation of Pt nanoparticles on carbon nanotubes by hydrothermal method. *Energy Conservation and Management*. **47**. 3235-3240 (2006).
- <sup>25</sup> Wang, X., Li, W., Chen, Z., Waje, M., Yan, Y. Durability investigation of carbon nanotube as catalyst support for proton exchange membrane fuel cell. *Journal of Power Sources*. **158**. 154-159 (2006).
- <sup>26</sup> Guha, A., Zawodzinski, T., Schiraldi, D. Surface-modified carbons as platinum catalyst support for PEM fuel cells. *Journal of Power Sources*. **172**. 530-541 (2007).
- <sup>27</sup> Lee, K., Zhang, J., Wang, H., Wilkinson, D. Progress in the synthesis of carbon nanotube- and nanofiber-supported Pt electrocatalysts for PEM fuel cell catalysis. *Journal of Applied Electrochemistry*. **36**. 507-522 (2006).
- <sup>28</sup> Liu, Z., Lin, Z., Lee, J., Zhang, W., Han, M., and Gan, L. Preparation and characterization of platinum-based electrocatalysts on multiwalled carbon nanotubes for proton exchange membrane fuel cells. *Langmuir*. **18**. 4054-4060 (2002).
- <sup>29</sup> Lordi, V., Yao, N., Wei, J. Method for supporting platinum on single-walled carbon nanotubes for a selective hydrogenation catalyst. *Chemical Materials*. **13**. 733-737 (2001).
- <sup>30</sup> Shaijumon, M., Rampaprabhu, S. Platinum/multiwalled carbon nanotubes-platinum/carbon composites as electrocatalysts for oxygen reduction reaction in proton exchange membrane fuel cell. *Applied Physics Letters*. **88**. 253105 (2006).
- <sup>31</sup> Zheng, S., Hu, J., Zhong, L., Wan, L., Song, W. In situ one-step method for preparing carbon nanotubes and Pt composite catalysts and their performance for methanol oxidation. *American Chemical Society* . 2007.

---

<sup>32</sup> Li, X., Liu, Y., Fu, L., Cao, L., Dacheng, W., and Wang, Y. Efficient synthesis of carbon nanotube-nanoparticle hybrids. *Advanced functional materials*. **16**. 2431-2437 (2006).

<sup>33</sup> Li, W., Wang, X., Chen, Z., Waje, M., and Yan, Y. Carbon nanotube film by filtration as cathode catalyst support for proton-exchange membrane fuel cell. *Langmuir*. **2005**. 9386-9389 (2005).